

1 **Long-term changes in explosive and effusive behaviour at andesitic arc volcanoes:**  
2 **chronostratigraphy of the Centre Hills Volcano, Montserrat**

3  
4 **Maya Coussens**

5 School of Ocean and Earth Science, National Oceanography Centre, University of  
6 Southampton, European Way, Southampton, SO14 3ZH, UK (mfc1e12@soton.ac.uk)

7  
8 **Michael Cassidy**

9 Institute of Geosciences, Johannes Gutenberg, University Mainz, J- J- Becher- Weg 21, D-  
10 55128, Mainz, Germany (mcassidy@uni-mainz.de)

11  
12 **Sebastian. F. L. Watt**

13 School of Geography, Earth and Environmental Sciences, University of Birmingham,  
14 Edgbaston, Birmingham, B15 2TT, UK (s.watt@bham.ac.uk)

15  
16 **Martin Jutzeler**

17 School of Physical Sciences (Earth Sciences), University of Tasmania, Private Bag 79,  
18 Hobart Tasmania 7001, Australia (jutzeler@gmail.com)

19  
20 **Peter. J. Talling**

21 National Oceanography Centre, Southampton, University of Southampton, Southampton  
22 SO14 3ZH, UK (peter.talling@noc.ac.uk)

23  
24 **Dan Barfod**

25 Scottish Universities Environmental Research Centre, Rankine Avenue, Scottish Enterprise  
26 Technology Park, East Kilbride, G75 0QF, UK (Dan.Barfod@glasgow.ac.uk).

27  
28 **Thomas. M. Gernon, Rex Taylor, Stuart. J. Hatter, Martin. R. Palmer**

29 School of Ocean and Earth Science, National Oceanography Centre, University of  
30 Southampton, European Way, Southampton, SO14 3ZH, UK  
31 (Thomas.Gernon@noc.soton.ac.uk), (rex@noc.soton.ac.uk), (sjh1e13@soton.ac.uk),  
32 (m.palmer@noc.soton.ac.uk)

33  
34 **and the Montserrat Volcano Observatory**

35 Mongo Hill, Montserrat, PO Box 318, Flemmings, Montserrat, West Indies

36  
37 **Abstract**

38 Volcanism on Montserrat (Lesser Antilles arc) has migrated southwards since ~2.5 Ma,  
39 forming three successively active volcanic centres. The Centre Hills volcano was the focus  
40 of volcanism from ~1–0.4 Ma, before activity commenced at the currently active Soufrière  
41 Hills volcano. The history of activity at these two volcanoes provides an opportunity to  
42 investigate the pattern of volcano behaviour on an andesitic arc island over the lifetime of  
43 individual volcanoes. Here, we describe the pyroclastic stratigraphy of subaerial exposures  
44 around central Montserrat, identifying 11 thick (>1 m) pumiceous units derived from  
45 sustained explosive eruptions of Centre Hills from ~0.8–0.4 Ma, and a similar number of  
46 less well exposed pumiceous deposits. The pumice-rich units are interbedded with  
47 andesitic lithic breccias derived from effusive, dome-forming eruptions of Centre Hills.  
48 The stratigraphy indicates that large (up to magnitude 5) explosive eruptions occurred  
49 throughout the history of Centre Hills, alongside effusive activity. This behaviour contrasts  
50 with Soufrière Hills, where deposits from sustained explosive eruptions are much less

51 common and are restricted to early stages of activity at the volcano, from ~175–130 ka.  
52 Subsequent eruptions at Soufriere Hills have been dominated by andesitic effusive  
53 eruptions. The bulk composition, petrography and mineral chemistry of volcanic rocks  
54 from Centre Hills and Soufrière Hills is similar throughout the history of both volcanoes,  
55 except for occasional, transient departures to different magma compositions, which mark  
56 shifts in vent location or dominant eruption style. For example, the final eruption of Centre  
57 Hills, before the initiation of activity at Soufrière Hills, was more silicic than any other  
58 identified eruption on Montserrat; and the basaltic South Soufrière Hills episode marked  
59 the transition to the current stage of predominantly effusive Soufrière Hills activity. The  
60 compositional stability observed throughout the history of Centre Hills and Soufrière Hills  
61 suggests that a predominance towards effusive or explosive eruption styles is not driven by  
62 major compositional shifts in the magma system, but may reflect local changes in long-  
63 term magma storage conditions that characterise individual episodes (on  $10^5$  year  
64 timescales) of volcanism on Montserrat.

## 65 66 **1. Introduction**

67 Individual volcanoes commonly exhibit different styles of eruptive behaviour through time,  
68 characterised by shifts in eruption style, frequency or composition (e.g., Druitt et al., 1989;  
69 Bacon and Lanphere, 2006; Singer et al., 2008; Germa et al., 2011), and potentially  
70 reflecting changes in magma genesis, processing and storage in the underlying plumbing  
71 system (e.g., Humphreys et al., 2006; Brown et al., 2014). Reconstructing long-timescale  
72 ( $10^3$ – $10^5$  year) patterns in volcanic behaviour can provide insights into the physical and  
73 chemical parameters that govern eruptive styles at a volcano, and how the processes  
74 driving volcanism may vary during the development of an individual volcanic system.

75  
76 The island of Montserrat, in the Lesser Antilles island arc, comprises three main volcanic  
77 centres and has been a site of active subaerial volcanism since at least 2.6 Ma. The most  
78 recent eruption of Soufrière Hills, from 1995 to 2010, involved the extrusion of andesitic  
79 lava domes, with periodic partial dome collapse and vulcanian explosions (Druitt and  
80 Kokelaar 2002; Wadge et al., 2014). This eruption and the underlying Soufrière Hills  
81 magma system have been extensively studied (e.g., Barclay et al., 1998; Edmonds et al.,  
82 2001; Devine et al., 2003; Humphreys et al., 2009), but relatively little is known about the  
83 earlier history of volcanism on Montserrat.  $^{40}\text{Ar}/^{39}\text{Ar}$  dating ((Harford et al., 2002; Brown  
84 and Davidson 2008) and stratigraphic studies (Rea et al., 1975; Baker et al., 1985; Wadge  
85 and Isaacs 1988; Roobol and Smith 1998; Smith 2007) indicate andesitic subaerial activity  
86 at Soufrière Hills since ~290 ka, dominated by effusive eruptions, and interrupted by a  
87 brief interlude of basaltic volcanism at the South Soufriere Hills at ~130 ka (Harford et al.,  
88 2002; Cassidy et al., 2015). Prior to this, current dates for subaerial activity at Centre Hills  
89 span the interval 0.95–0.55 Ma, and 2.6–1.2 Ma for Silver Hills, the oldest volcanic centre  
90 on Montserrat (Figure 1). Volcaniclastic deposits within the offshore sedimentary  
91 stratigraphy (e.g., Watt et al., 2012; Trofimovs et al., 2013) provide a more complete  
92 record of volcanic activity at Montserrat (Coussens et al., 2016), and suggest a more  
93 continuous level of volcanism than indicated by dated subaerial units (which imply gaps on  
94  $10^4$ -year timescales between activity at the individual volcanic centres). However, many of  
95 these offshore deposits are mixed volcaniclastic turbidites, potentially derived from a range  
96 of primary volcanic processes (e.g. Trofimovs et al., 2013; Cassidy et al., 2014a). Eruption  
97 style is thus difficult to determine from the marine stratigraphy, but is more easily assessed  
98 from proximal subaerial exposures of volcaniclastic deposits.

99

100 This paper provides the first description of the onshore stratigraphy in the central part of  
101 Montserrat, based mainly on exposures along the east and west coasts. These deposits are  
102 mostly of Centre-Hills age, and we compare the stratigraphic record obtained with that of  
103 Soufrière Hills. By producing a record of volcanism on Montserrat since ~1 Ma, we aim to  
104 document the timing of major phases of activity, to determine how the style of volcanism  
105 has varied over this period, and to assess whether this variation followed consistent trends  
106 during the development of the Centre Hills and Soufrière Hills magmatic systems.

107

## 108 **2. Methods**

109 Past stratigraphic studies (e.g., Roobol and Smith, 1998; Harford et al., 2002) show that  
110 individual eruptions on Montserrat have involved a range of processes, including effusive  
111 activity, partial lava-dome collapses (generating pyroclastic density currents (PDCs)),  
112 short-lived vulcanian explosions, and more sustained explosive eruptions. The latter type  
113 of activity produces relatively widespread, pumice-rich tephra-fall and PDC-derived  
114 deposits, forming extensive stratigraphic horizons that can be correlated based on physical  
115 or chemical characteristics (e.g., Lowe 2011). These widespread pyroclastic deposits can  
116 be used to construct local stratigraphic frameworks, defining discrete episodes of activity  
117 at the volcano. To investigate the volcanic stratigraphy exposed in the central part of  
118 Montserrat we therefore focus principally on pumice-rich units, which have more potential  
119 for inter-site correlation and ultimately for correlating between subaerial exposures and the  
120 marine sedimentary record.

121

### 122 **2.1 Fieldwork**

123 Fieldwork was conducted in February 2013, investigating exposures in road cuttings and  
124 coastal cliffs throughout the central region of Montserrat (Figure 1). Areas affected by the  
125 1995-2010 eruption of Soufrière Hills, as well as the northernmost part of the island, where  
126 the oldest rocks on Montserrat are exposed around the deeply eroded Silver Hills volcano,  
127 were excluded from this study. The study area is therefore broadly centred around the  
128 Centre Hills volcano, which consists of three steep-sided hills that merge together to form  
129 the central peak of Katy Hill, where exposed blocky lavas are likely to represent the  
130 approximate site of the main Centre Hills vent (Harford et al., 2002). Centre Hills is cut by  
131 several steep valleys. This part of the island is densely forested, and inland exposure is  
132 poor and limited to a few road cuttings. The coastal cliffs provide much more extensive  
133 exposures, typically ranging from 10 m to 50 m in height on the west coast, and 30 m to  
134 100 m on the east coast (Figure 1).

135

136 The exposures studied here preserve proximal facies, with depositional patterns controlled  
137 by local topography, and widespread erosion affecting deposit preservation. Exposures are  
138 often laterally discontinuous, hindering stratigraphic correlation between sites. Pumice-rich  
139 pyroclastic deposits provided the most distinct units (in terms of physical appearance and  
140 sedimentological characteristics) and the correlation between sites across the island. Field  
141 correlation of pyroclastic deposits thus forms the basis of the stratigraphy presented here.  
142 Bulk and glass chemical analyses (Section 2.2) were used to resolve ambiguities in the  
143 field-based stratigraphy and to test correlations.

144

145 Many of the pyroclastic deposits studied here are internally complex, but where deposits  
146 appear as a continuous stratigraphic sequence, dominated by juvenile pyroclastic material  
147 with similar characteristics (e.g. colour, phenocryst assemblage), they have been grouped  
148 together as a single eruptive unit. It is inferred that each of these units were formed during  
149 one eruption, albeit with potential variation in eruption style.

150

151 Approximately 15 km of coastal exposures and 8 road cuttings were logged around  
152 Montserrat, recording the physical appearance, structure, mineralogical and  
153 sedimentological characteristics of individual deposits. Pumiceous deposits were sampled  
154 for chemical analysis, and maximum lithic and pumice clast sizes were estimated by  
155 measuring the mean of the orthogonal axes of the three largest clasts found within a 10-  
156 meter length outcrop. Deposits were described using the terminology outlined by White  
157 and Houghton (2006), and PDC deposits identified using criteria outlined in Branney and  
158 Kokelaar (2002). In some sections, weathering (discolouration and clay alteration) affected  
159 the appearance of exposures, and since we cannot be certain if outcrops preserve original  
160 textures, we do not distinguish between consolidated and unconsolidated units (ash is thus  
161 used only as a grain-size (<2 mm) description).

162

## 163 2.2 Whole rock Chemistry

164 Lapilli-sized pumice clasts were collected from most of the identified pumiceous units,  
165 with some additional sampling of lithic clasts and ash deposits. Fresh clasts (i.e. showing  
166 no visible evidence of alteration or discolouration; this was possible for all pumiceous  
167 units except the Angry Bird pumice) were selected for bulk chemical analysis of major  
168 (XRF; Philips Magix Pro wavelength- dispersive XRF at the National Oceanography  
169 Centre, Southampton) and trace (XRF and ICP-MS; VG Plasmaquad PQ2 p at the National  
170 Oceanography Centre, Southampton) elements. Samples were rinsed, dried and crushed  
171 before being ground to a fine powder using a tungsten carbide mill. Powder pellets and  
172 glass beads were prepared for XRF analysis, using the JA-1, BCR1, and BE-N standards.  
173 For ICP-MS, 0.05g of powder was dissolved in 3% HNO<sub>3</sub> and 3% HF, and then dried and  
174 re-dissolved with ~5 g HCl topped up to 10 g with MilliQ Water. 0.5 ml of this solution  
175 was then extracted and dried overnight. The residue was then re-dissolved, and made up to  
176 a 10 g solution with 3% HNO<sub>3</sub> solution with 5 ppm of indium and rhenium to achieve a  
177 dilution factor of 4000. Precision for all elements was generally better than 2%, except for  
178 Ni and Cs where precision was better than 6% RSD (see Supplementary Data).

179

## 180 2.3 Mineral and glass compositions

181 Mineral and glass chemistry were analysed in juvenile clasts from all pumiceous units. For  
182 mineral chemistry a Leo 1450VP scanning electron microscope (SEM) with an Oxford  
183 Instruments X-Act 10 mm<sup>2</sup> silicone drift detector and energy dispersive spectroscopy was  
184 used at the National Oceanography Centre, Southampton. Beam current was 10 nA with an  
185 analysis time of 180 seconds. Haematite and clinopyroxene standards were used to check  
186 for instrument drift and calibration. All analyses presented here have been normalised to  
187 100 wt.% anhydrous compositions. Standard deviation of results is generally <0.4 wt.%  
188 (raw data are provided in Supplementary Tables).

189

190 Glass chemistry was analysed using a Cameca SX100 microprobe at the Department of  
191 Earth Sciences, University of Bristol. A beam current of 4 nA was used with a beam  
192 diameter of 5 µm and an analysis time of 180 seconds. Each samples was analysed  
193 multiple times. Any totals of <95 wt.% were discarded. Pumice clasts from several  
194 separate locations were analysed to test stratigraphic correlations (raw data are provided in  
195 Supplementary Tables).

196

## 197 2.4 <sup>40</sup>Ar/<sup>39</sup>Ar dating

198 A small number of pumiceous units were selected for <sup>40</sup>Ar/<sup>39</sup>Ar dating. The glassy  
199 groundmass of these pumices was unsuitable for dating, and plagioclase phenocrysts were

200 therefore picked out for dating. It is possible that results may be biased towards older ages  
201 due to xenocrystal plagioclase (cf. Harford et al., 2002). Samples were crushed using a jaw  
202 crusher and then wet sieved and left to dry overnight. Plagioclase crystals were separated  
203 from sieved fractions of 125-250  $\mu\text{m}$  and 250-500  $\mu\text{m}$  using a model LB-1 Frantz magnetic  
204 separator. Separated crystals and neutron flux monitors were placed in copper foil packets  
205 and stacked in quartz tubes. The sample package was irradiated for 2.0 hours in the Oregon  
206 State University reactor, Cd-shielded facility. Gas was extracted from samples using either  
207 an all-metal resistively-heated furnace or a mid-infrared (10.6  $\mu\text{m}$ )  $\text{CO}_2$  laser. Liberated  
208 argon was then purified of active gases (e.g.,  $\text{CO}_2$ ,  $\text{H}_2\text{O}$ ,  $\text{H}_2$ ,  $\text{N}_2$ ,  $\text{CH}_4$ ) using three Zr-Ti-Al  
209 getters; one at 16°C and two at 400°C. Data were collected on a GVi instruments ARGUS  
210 V multi-collector mass spectrometer using a variable sensitivity Faraday collector array in  
211 static collection mode. The reader is directed to Harford et al. (2002) for full details of this  
212 approach. The Ar-Ar dates have relatively large errors, with 2  $\sigma$  errors  $< \pm 0.2$  Ma, due to  
213 the low K content of Montserrat's eruptive products.  
214

### 215 **3. Results**

#### 216 3.1 Volcanic stratigraphy

217 The stratigraphy of volcanic deposits exposed in central Montserrat is summarised in this  
218 section. The stratigraphy has been developed primarily from field relationships, with some  
219 refinements based on bulk or glass chemistry.  
220

221 Exposures throughout the study area comprise a mixture of pumice-rich deposits (with  
222 individual thicknesses of up to 16 m, but generally less) interbedded with generally thicker  
223 deposits of dense andesitic lithic breccias (often  $>10$  m in thickness) (Figures 2 to 4).

224 Pumiceous units are frequently lenticular and laterally discontinuous, with eroded upper  
225 surfaces cross-cut by the deposition of younger lithic-rich deposits. As such, the full  
226 primary thickness of pumiceous units is not always preserved. Lithic breccias have similar  
227 physical characteristics throughout the area, being dominated by poorly sorted, angular  
228 dense grey andesite blocks. Individual deposits have lateral extents of tens to hundreds of  
229 metres, with poorly developed grading or internal bedding. The lateral variation and  
230 similar appearance of lithic units throughout the area hinders their direct correlation  
231 between sites. The lithic breccias may represent primary or secondary deposits associated  
232 with lava-dome forming eruptions, as well as non-eruptive mass wasting and alluvial  
233 processes. Although they cannot be correlated directly, packages of lithic units can be  
234 defined by their bounding pumiceous deposits, which are more easily correlated between  
235 sites due to their more distinctive appearance and widespread nature (particularly tephra  
236 fall deposit components).  
237

238 Pumiceous units to the northeast and southwest of Centre Hills can often be traced laterally  
239 in cliff exposures for several hundred metres. To the west, northwest and southeast, more  
240 extensive localised erosion has produced less laterally continuous deposits, with channels  
241 filled with lithic breccias truncating pyroclastic units through erosive discordances. In total,  
242 twenty four individual pumice-rich units have been identified based on their physical  
243 appearance, stratigraphic order and chemistry. Many of these units are poorly exposed and  
244 only recognised from a single site (these units are often relatively thin ( $<1$  m)). The poor  
245 preservation of several units suggests that our stratigraphy is likely to be incomplete, with  
246 the products of smaller explosive eruptions having little or no representation in subaerial  
247 exposures. Twelve of the identified pumiceous units are relatively more laterally extensive  
248 or thicker, and have been investigated in more detail. Many of these have been correlated  
249 across multiple sites (Figures 2 and 3) and used to produce a local stratigraphic framework.

250 A brief description of each of these units is given below, in approximate stratigraphic order,  
251 with more detailed lithofacies descriptions in Table 1.

252

### 253 3.1.1 Exposures west of Centre Hills

254 Cliff exposures along the west coast of Montserrat are more extensive than on the east, and  
255 preserve a larger number of pyroclastic deposits, even though the cliffs are generally  
256 higher on the east coast. We therefore describe units exposed west of Centre Hills first.

257 In general, the thickest pumiceous deposits are found east of Katy Hill (Figure 1) and have  
258 a thinning pattern that is consistent with a provenance from Centre Hills. This is less clear  
259 for the Bransby Point and Garibaldi Hill pumices, which could potentially be derived from  
260 a more southerly vent site. The wide submarine shelf around Bransby Point (Figure 1)  
261 suggests that this southern part of the island is older than Soufrière Hills (which has a very  
262 narrow submarine shelf), and it is possible that older volcanic vents in this region are now  
263 buried beneath younger volcanic rocks. However, the small number of field sites makes it  
264 difficult to identify vent sites precisely for any of these units.

265

266 Only one unit, the Old Road Bay pumice, was found both east and west of Centre Hills.

267 The relative age of east- and west-coast deposits above and below this tie point is thus  
268 uncertain, but has been investigated by  $^{40}\text{Ar}/^{39}\text{Ar}$  dating (Section 3.3).

269

270 To the southwest of Centre Hills, five extensive pumice-rich units (Old Road Bay pumice,  
271 Garibaldi Hill pumice, Bransby Point pumice, Old Road Bay tuff, and Foxes Bay pumice)  
272 overlie the less well exposed South Lime Kiln Bay pumice. To the northwest of Centre  
273 Hills, three stratigraphically younger units are well exposed (the Bunkum Bay pumice,  
274 Woodlands Bay pumice, and the Attic pumice).

275

#### 276 *South Lime Kiln Bay pumice*

277 The South Lime Kiln Bay pumice crops out within a faulted block at Lime Kiln Bay  
278 (southwest of Katy Hill) that exposes relatively older strata. In this area the exposure is a  
279 pumice-dominated medium-lapilli deposit, >7 m in total thickness and divided into three  
280 units (Table 1). Decimetre- to metre-scale beds of pumice (90% pumice), with variable  
281 sorting, are interbedded with thin medium-coarse grained ash beds and lithic-rich intervals.  
282 The full unit is interpreted as a sequence of tephra fall and high-concentration PDC  
283 deposits. The proportion of lithic clasts increases in the uppermost part of the unit.

284

#### 285 *Old Road Bay pumice*

286 The Old Road Bay pumice has been identified across several sites and is the only unit  
287 identified in coastal exposures both east and west of Centre Hills (Figures 2 and 3),  
288 forming one of the stratigraphically oldest deposits on the west coast. It comprises a series  
289 of pumice-rich (up to 80 vol.%) lapilli-tuff deposits with lenses of well-sorted pumice  
290 lapilli and discontinuous ash-rich horizons, with a total thickness of up to 6 m divided into  
291 three units (Table 1). The lower units preserve occasional low-angle bedding, with the  
292 middle unit comprising banded beds of ash and lapilli, with accretionary lapilli in places.  
293 They are interpreted as the reworked (i.e. partially rounded) products of fall deposits from  
294 pulsatory explosive activity and/or low concentration PDC deposits. The uppermost unit  
295 comprises the bulk of the deposit and is more massive, poorly sorted mixture of pumice  
296 and lithic clasts, interpreted as the product of a high-concentration PDC. Pumices  
297 throughout the deposit are buff coloured and the cement weathers to a distinctive pink-  
298 orange colour.

299

300 *Garibaldi Hill pumice*

301 The Garibaldi Hill pumice has a total thickness of up to 5.5 m, forming a coarse lapilli  
302 pumice that crops out to the south west of Centre Hills, where it comprises a lower unit of  
303 poorly sorted lapilli tuff, interpreted as a high-concentration PDC deposit, capped by an  
304 upper massive unit of well sorted angular pumice lapilli (95 vol.% pumice), interpreted as  
305 a fall deposit (Table 1). The unit thins northwards into a laminated grey tuff with a  
306 distinctive pink tuff top. The deposit is well exposed around Garibaldi Hill, where it has  
307 been locally uplifted and tilted.

308

309 *Bransby Point pumice*

310 The Bransby Point pumice is laterally continuous over a distance of 3 km in the SW part of  
311 Montserrat at Bransby Point and Foxes bay, thinning northwards. It has a distinctive grey  
312 and pink colour, and can be divided into two units of similar thickness (2 m total thickness).  
313 Both units contain well sorted, angular pumice lapilli. The lower bed is white to grey in  
314 colour, with faint internal stratification on a decimetre scale. It is capped by a thin (<10  
315 cm) pink ash. The upper unit is more massive, containing pink pumices, with  
316 discontinuous 1-cm thick ash horizons, capped by a 5 cm ash deposit. The beds are  
317 interpreted as fall deposits from a sustained explosive eruption.

318

319 *Old Road Bay tuff*

320 This unit forms a distinctive ash-rich marker beds that can be traced widely along the west  
321 coast of Montserrat, with a total thickness of up to <1 m divided into two sub-units (Table  
322 1). The lower bed is a well sorted laminated tuff, grey at the upper and lower margins and  
323 yellow in the centre and faintly bedded on a decimetre scale. The upper bed has a more  
324 variable thickness and is coarser, bedded on a centimetre scale and comprising yellow ash  
325 beds and thin (single clast thickness) pumice fine-lapilli beds. The lateral continuity and  
326 sorting of the lower bed suggests an origin as a fall deposit, while the upper part may result  
327 from a low-concentration PDC associated with unsteady explosive eruption.

328

329 *Foxes pumice*

330 The Foxes pumice is poorly exposed at a single site on the SW coast of Montserrat, but  
331 forms a thick (3.2 m), well-sorted pumice-rich deposit (Table 1). The lowermost part is a  
332 well sorted, pink medium-ash deposit, with faint lamination, overlain by a massive 3-m  
333 thick well-sorted angular pumice (>90 vol%) pumice lapilli deposit, with faint decimetre-  
334 scale bedding. The unit is interpreted as a fall deposit from a large sustained explosive  
335 eruption.

336

337 *Bunkum Bay pumice*

338 The Bunkum Bay pumice crops out only at Bunkum Bay, forming a series of overlapping  
339 channels of alternating orange-brown lapilli-tuff and tuff beds (Figure 4c), exceeding 3 m  
340 in thickness and comprising poorly sorted ash-rich beds with variable proportions of  
341 pumice and lithic clasts, including horizons rich in accretionary lapilli (Table 1). Some  
342 beds show low angle bedding and reverse grading, and the sequence is interpreted as the  
343 product of unsteady high-concentration pyroclastic density currents. This part of the  
344 deposit is overlain by a massive 7-m thick polymict deposit which was inaccessible for  
345 direct examination but may reflect reworking (e.g. lahar deposits) of deposits from the  
346 same eruption.

347

348 *Woodlands Bay pumice*

349 The Woodlands Bay pumice is one of the coarsest and thickest pumiceous deposits

350 exposed on Montserrat, with a total thickness of up to 16 m. The lower parts of the unit  
351 comprise variably sorted beds on metre- to decimetre-scales, dominated by buff-coloured  
352 pumice but with some lithic rich horizons and cross-bedded lenses, interpreted as the  
353 product of high-concentration PDCs (Table 1). The is overlain by a thick central sequence  
354 of pumice-rich (70-90 vol.%) moderately-well sorted lapilli beds on metre- to decimetre-  
355 scales, with a mean pumice clast size of 2-4 cm and maximum size of 11 cm. These coarse  
356 lapilli beds are interspersed with more ash-rich (< 40 vol.%) pumice lapilli beds. The  
357 central part of the unit is interpreted as tephra fall deposits, potentially partially reworked,  
358 interleaved with pumice-rich PDC deposits. This is overlain by an upper sequence of  
359 slightly coarser but more thinly bedded (decimetre scale) moderately- to well-sorted  
360 pumice lapilli beds (mean pumice clast size of 4.5 cm; maximum size of 18 cm) interpreted  
361 as fall deposits derived from powerful sustained explosive activity, with slight fluctuations  
362 in intensity. The Woodlands Bay pumice crops out at several sites in west and north-west  
363 of Montserrat.

364

#### 365 *Attic pumice*

366 The Attic pumice is the youngest of the pumiceous deposits studied here, and is best  
367 exposed in road cuttings on the west side of Montserrat, forming a 3-m thick sequence of  
368 white, metre-scale fine-lapilli tuffs, with abundant ash-coated pelletal pumice grains  
369 (Figure 4e). The lower part of this unit has planar laminations in places, while the upper  
370 section is cross-bedded, coarser and more poorly sorted, with some relatively larger lithic  
371 clasts. It overlies a thicker (up to 3-m) bed of medium-coarse lapilli-tuff that is poorly  
372 exposed. This unit has fewer pelletal grains, particularly near the based, and contains  
373 lenses of coarse pumice lapilli with some bedding structures (Table 1). The entire sequence  
374 is interpreted as the product of wet low- to moderate-concentration PDCs.

375

#### 376 3.1.2 Exposures east of Centre Hills

377 Four pumiceous units are well exposed on cliff sections east of Centre Hills (there are few  
378 road cuttings in this area). One of these, the Old Road Bay pumice, also occurs west of  
379 Centre Hills and is described above. The Old Road Bay pumice lies above the Angry Bird  
380 pumice, and at a similar stratigraphic level to the Bramble pumice (their relative age  
381 cannot be deduced from field exposures). Above these, the youngest unit on the east coast  
382 is the Statue Rock pumice.

383

#### 384 *Angry Bird pumice*

385 The Angry Bird pumice crops out only on the east coast of Montserrat near Bramble  
386 Airport and around Statue Rock. It lies stratigraphically below the Old Road Bay pumice.  
387 The unit comprises up to four massive pumice-rich lapilli deposits, which are truncated by  
388 massive lithic-rich channel-fill deposits. Pumices are 1-2 cm in diameter, angular to sub-  
389 angular with a flattened shape, and are altered to soft clays (Table 1). The beds have a pink  
390 ash matrix (10 vol.%) and infrequent lithic clasts (1 cm; 5 vol.%). Beds thin northwards,  
391 and are laterally continuous over several hundred metres. The beds are interpreted as  
392 tephra fall deposits, with the lithic sequences perhaps reflecting mass-wasting deposits  
393 derived from associated effusive activity. The lowermost pumice bed directly overlies a  
394 glassy porphyritic (35 vol% plagioclase; 15 vol.% pyroxene) lava flow at the Bramble  
395 Airport exposures.

396

#### 397 *Bramble pumice*

398 The Bramble pumice is poorly preserved on the east coast as thin (cm-thicknes; ~10 m  
399 lateral extent) bands or lenses within a 12-m thick sequence of massive andesitic lithic

400 breccias (Table 1). The unit also contains a bed of distinctive slab-shaped rip-up clasts of  
401 laminated ash. The pumiceous component of the unit appears to be largely reworked, and it  
402 is difficult to assess the characteristics of the primary eruption deposit.

403

#### 404 *Statue Rock pumice*

405 The Statue Rock pumice is a poorly sorted lapilli-tuff with a matrix of yellow coarse  
406 crystalline ash, with localised lenses of lithic breccia and pumice lapilli. The overall unit  
407 displays low angle cross bedding and has a laterally variable thickness of ~10 m (Table 1).  
408 The unit crops out on the west coast at Statue Rock and can be traced along the cliff  
409 section for ~1 km. We interpret the unit as partially reworked deposits of high-  
410 concentration PDCs.

411

### 412 3.2 Chemistry and petrography

413 The pyroclastic units described above were defined using field relationships. We have  
414 analysed the bulk pumice chemistry of each of these units, and in some cases have used  
415 additional glass and mineral analyses to test field correlations. We identified no evidence  
416 of compositional heterogeneity in the juvenile products of any of the deposits studied here  
417 (i.e. changes in the colour, mineral content and phase assemblage of pumice clasts),  
418 suggesting that the magma erupting in each event was compositionally homogeneous. This  
419 is supported by glass analyses from individual units sampled across several sites, which  
420 form distinct clusters in their major-element chemistry. The bulk chemistry of all  
421 pumiceous units analysed here is broadly similar, but there is sufficient compositional  
422 variation to discriminate between individual units.

423

#### 424 3.2.1 Major element chemistry

425 The bulk pumice silica composition (Table 2) lies between 58 and 63 wt.% for all the units  
426 studied here, defining them as andesites, except for the Attic pumice (the youngest unit),  
427 which is slightly more silicic (65.4 wt.% SiO<sub>2</sub>; dacite), and the Angry Bird pumice (52.3  
428 wt.% SiO<sub>2</sub>; basaltic andesite) (Figure 5). The latter is the stratigraphically oldest deposit  
429 here (alongside the South Lime Kiln bay pumice; their relative age cannot be deduced),  
430 and is also the only deposit where the pumices were extensively altered to clay minerals.  
431 This alteration may have potentially affected its bulk chemistry, although its overall major  
432 element contents are not atypical for basaltic andesites, and lie on consistent fractionation  
433 trends with the andesitic units. Notwithstanding the potential effects of alteration, the  
434 Angry Bird pumice therefore appears to be distinctively more mafic than the other units  
435 studied here (Figure 5). Analyses of seven additional un-named pumiceous units (Table 2)  
436 also fall within the andesitic compositional range above (one sample is very slightly more  
437 mafic, at 56.8 wt% SiO<sub>2</sub>), suggesting that nearly all the large explosive eruptions from  
438 Montserrat throughout the studied stratigraphic period erupted andesitic magmas.

439

440 All samples lie on tholeiitic and medium K-series trends (<1 wt.% K<sub>2</sub>O), forming a linear  
441 compositional array where the observed chemical variation can be attributed to fractional  
442 crystallisation processes (Figure 5). These compositions are similar to previously reported  
443 data for lavas from Centre Hills and Silver Hills (56–64 wt.% SiO<sub>2</sub>) (Zellmer et al., 2003),  
444 although both the Angry Bird and Attic pumices fall outside this previously recognised  
445 compositional range. If all the units are placed in stratigraphic order (Figure 6), there is no  
446 apparent temporal variation in major element compositions except for a general trend  
447 towards more potassic compositions in younger units (the Statue Rock pumice lies off this  
448 trend). The Attic pumice is the most chemically evolved unit studied and is easily  
449 discriminated from the other units by its bulk composition. The other units cannot easily be

450 distinguished on the basis of major element bulk composition.

451

### 452 3.2.2 Trace element chemistry

453 Whole-rock trace element compositions of pumices (Table 3) show more inter-unit  
454 variation than major element compositions and can be used to distinguish between units.  
455 For example, Nd and Y compositions (Figure 7) cluster tightly for individual deposits,  
456 defining discrete compositional ranges that can be used for inter-site correlation. Plotting  
457 the units in stratigraphic order (Figure 6) indicates long-term trends towards relative HREE  
458 depletion in the younger units (i.e. higher La/Lu ratios) and enrichment in high field-  
459 strength elements such as Th. The more evolved Attic pumice again has compositions (e.g.  
460 high Ba contents) that distinguish it from the other units. The low Ba content of the Angry  
461 Bird pumice may reflect its extensive alteration, resulting in low concentrations of mobile  
462 elements.

463

464 Lavas from Centre and Silver Hills have a relatively lower Ba/La ratio compared to the  
465 Soufrière-South Soufrière Hills volcanic complex (Cassidy et al., 2012). This relationship  
466 can be used to test our stratigraphic inference, based on the general thickening of  
467 pyroclastic deposits within the central part of Montserrat, that most of the units identified  
468 here are derived from Centre Hills. All the samples analysed here (all named units except  
469 Bransby point, and nine additional un-named units (Table 3)) form a clustered group with  
470 slightly lower Ba/La than Soufrière Hills (Figure 8), overlapping with previous  
471 Centre/Silver Hills data, but displaced slightly to higher Th/La values. This supports an  
472 origin from Centre or Silver Hills for these units.

473

### 474 3.2.3 Mineral and glass chemistry

475 Pumices from all the studied units are, like Montserrat's andesitic lavas, highly porphyritic,  
476 with phenocryst contents ranging from 20 to 50 vol.%. The typical phenocryst assemblage  
477 in all the studied units is plagioclase + hypersthene + Fe-Ti oxides ± augite/low Fe  
478 diopside ± quartz. The Attic pumice (the most silicic and youngest unit) is also  
479 mineralogically distinctive, with a phenocryst assemblage of hypersthene + hornblende +  
480 plagioclase + quartz. With the exception of the Attic pumice, the absence of phenocryst  
481 hornblende distinguishes the studied units from the magmas erupting at Soufrière Hills  
482 since ~130 ka, which have hornblende as a phenocryst phase (cf. Harford et al., 2002;  
483 Cassidy et al., 2015).

484

485 Pyroxene phenocrysts showed no significant compositional zoning within the analysed  
486 units. Orthopyroxene phenocrysts are Fe-rich hypersthene with core compositions of  $\text{Fs}_{33-38}\text{En}_{59-65}\text{Wo}_{1-5}$  (n=30) and very similar rim compositions of  $\text{Fs}_{34-38}\text{En}_{60-64}\text{Wo}_{1-2}$  (n=29)  
487 compositions (Figure 9). Clinopyroxene phenocrysts are mostly low-Fe diopside or high-  
488 Ca augite with core compositions of  $\text{Fs}_{15-18}\text{En}_{39-41}\text{Wo}_{43-44}$  (n=32) and rim compositions of  
489  $\text{Fs}_{15-18}\text{En}_{38-41}\text{Wo}_{43-47}$  (n=27) (Figure 9). Plagioclase phenocrysts are varied and complex,  
490 exhibiting oscillatory, normal and reverse zoning spanning a range of relatively anorthitic  
491 compositions (core compositions of  $\text{An}_{77-91}$  (n=34) and rim compositions of  $\text{An}_{79-94}$   
492 (n=28)). The amphibole phenocrysts in the Attic pumice are classified as magnesio-  
493 hornblende based on their aluminium content.

494

495  
496 Orthopyroxene crystals show trace variations in chemistry between the major stratigraphic  
497 units from Centre Hills (Figure 9). Subtle variations in the Fe and Al content in the rims of  
498 orthopyroxene phenocrysts occur between different units, and can distinguish units with  
499 very similar bulk chemical compositions (e.g. the Attic and Bramble pumices; Figure 9).

500 Orthopyroxene rim chemistry may thus be a further characteristic (alongside bulk trace  
501 element and glass compositions) that has potential for deposit correlation, particularly  
502 when tying these subaerial deposits with the offshore stratigraphy.

503

504 Groundmass glass chemistry is widely used to characterise tephra fall deposits for  
505 chemical correlation (Lowe 2011), and was measured by EPMA on samples with no  
506 visible alteration (the Angry Bird pumice was therefore not analysed, and the Bunkum Bay  
507 deposit was also excluded based on the scatter shown in its K<sub>2</sub>O glass contents). Samples  
508 typically formed tightly clustered K<sub>2</sub>O compositions, suggesting that glass chemistry was  
509 invariant during individual eruptions. All units have broadly similar, rhyolitic glass  
510 compositions (70-80 wt.% SiO<sub>2</sub>), with small variations in TiO<sub>2</sub>, K<sub>2</sub>O and MgO (Figure 10)  
511 that define distinct field for a few units (Bransby Point, Foxes and Attic pumices), but  
512 largely overlapping fields for all other units. The Bransby Point pumice is distinctive in  
513 having a high glass K<sub>2</sub>O content (~2.5 wt.%).

514

515 From the small amount of data collected here, pre-eruptive magma storage temperatures  
516 can be estimated using amphibole, orthopyroxene-liquid, clinopyroxene-liquid, and  
517 plagioclase-liquid geothermobarometry. This is not intended to be a comprehensive survey,  
518 but indicates the broad temperature ranges of magmas feeding the eruptions studied here  
519 and can be used to compare with data from Soufrière Hills. Analyses are based on  
520 phenocryst and co-existing glass compositions (Ridolfi et al., 2010; Putirka et al., 2003,  
521 2005, 2008). Different geothermometers have been used depending on the phases present,  
522 and the results of different methods cannot necessarily be directly compared. For the Attic  
523 pumice, amphibole geothermometry indicates temperatures of 812–852°C (n=10). Higher  
524 temperatures are derived from an orthopyroxene-melt geothermometer for the South Lime  
525 Kiln Bay pumice (947–1080°C (n=13)) (note that orthopyroxene rims could not be used  
526 for any other units, because they did not pass a melt equilibrium test based on Kd<sub>(Fe-Mg)</sub>).  
527 Analyses from other units (see Supplementary Data tables) using a clinopyroxene-melt  
528 geothermometer (conducted on rims that pass the Kd<sub>(Fe-Mg)</sub> equilibrium test) indicate a  
529 slightly cooler but similarly broad temperature range of 894–1022°C (n=7) (using pressure  
530 independent equations from Putirka et al. (1996)). Slightly higher temperatures are  
531 produced by plagioclase-melt geothermometry (1003–1032°C; n=17) (plagioclase rims  
532 only, passing a Kd<sub>(Ab-An)</sub> equilibrium test) (Putirka et al., 2005).

533

### 534 3.3 Ages

535 Both stratigraphic thickening patterns and trace element chemistry suggest that the units  
536 studied here are derived from Centre Hills, although it is possible that some of the basal  
537 stratigraphic units (South Lime Kiln Bay and Angry Bird pumices) originate from Silver  
538 Hills (trace element chemistry cannot distinguish the two sources), or that some of south-  
539 western units (Bransby Point and Garibaldi Hill pumices), based on tephra fall deposit  
540 distribution, could originate from a slightly more southerly vent site. The age of the  
541 stratigraphy studied here has been investigated further by <sup>40</sup>Ar/<sup>39</sup>Ar dating, providing direct  
542 dates for six units (Figure 11). Previous <sup>40</sup>Ar/<sup>39</sup>Ar dates for Centre Hills span 0.95–0.55 Ma  
543 (Harford et al., 2002), and 2.6–1.2 Ma for Silver Hills (Harford et al., 2002; Brown and  
544 Davidson, 2008).

545

546 The stratigraphically oldest units identified here are the Angry Bird and South Lime Kiln  
547 Bay pumices. The Angry Bird pumice was too altered to be suitable for dating, but  
548 <sup>40</sup>Ar/<sup>39</sup>Ar analysis for the South Lime Kiln Bay pumice, using plagioclase phenocrysts,  
549 indicates an age of 1.31 ± 0.21 Ma (Figure 11; all errors quoted at 2σ level). This overlaps

550 with the youngest end of the known period of activity at Silver Hills (Harford et al., 2002),  
551 which is thus the likely source for this unit. Unlike the South Lime Kiln Bay pumice,  
552 which occurred in an isolated faulted block, the Angry Bird pumice can be related  
553 stratigraphically to the rest of the units studied here, since it lies just a few metres below  
554 the Old Road Bay pumice (Figure 2). The Old Road Bay pumice is exposed on both the  
555 east and west coasts and has a thickening pattern that suggests an origin from Centre Hills.  
556 This is confirmed by an  $^{40}\text{Ar}/^{39}\text{Ar}$  age of  $0.70 \pm 0.14$  Ma, which overlaps with the central  
557 stage of previously-dated Centre Hills volcanism (Harford et al., 2002). Given this age, we  
558 infer that the underlying Angry Bird pumice is also of Centre-Hills age.

559  
560 Stratigraphically above the Old Road Bay pumice lies the Garibaldi Hill and Bransby Point  
561 pumices. The latter has an  $^{40}\text{Ar}/^{39}\text{Ar}$  age of  $0.79 \pm 0.17$  Ma. Although this is older than the  
562 Old Road Bay pumice date, the dates are stratigraphically consistent if the relatively large  
563 dating errors are taken into account. The similar ages obtained for the Old Road Bay and  
564 Bransby Point pumices suggests that this stage of Centre Hills volcanism (~0.8-0.6 Ma)  
565 was characterised by several large explosive eruptions (Angry Bird, Old Road Bay,  
566 Bramble, Garibaldi Hill and Bransby Point pumices, as well as a number of un-named  
567 interbedded deposits, and followed by the stratigraphically younger but undated Old Road  
568 Bay tuff, Statue Rock pumice and Foxes pumice).

569  
570 The Bunkum Bay, Woodlands Bay and Attic pumices crop out extensively west and  
571 northwest of Centre Hills, and form a younger stratigraphic package.  $^{40}\text{Ar}/^{39}\text{Ar}$  ages are  
572  $0.51 \pm 0.11$  Ma for the Bunkum Bay pumice,  $0.59 \pm 0.11$  Ma for the Woodlands Bay  
573 pumice, and  $0.48 \pm 0.20$  Ma for the Attic pumice. Within error, these ages are again  
574 consistent with stratigraphic order, and suggest that these three eruptions all originated  
575 from Centre Hills at ~0.5 Ma.

576  
577 The distinct stratigraphic distribution of the three youngest units studied here (Bunkum  
578 Bay, Woodlands Bay and Attic pumices) suggests that they may represent a separate phase  
579 of volcanism at Centre Hills, but within the error of the  $^{40}\text{Ar}/^{39}\text{Ar}$  dates there is no evidence  
580 of a significant pause in explosive volcanism at Centre Hills. The ages indicate that at least  
581 eleven explosive eruptions (or at least 22, taking into account un-named and uncorrelated  
582 deposits) originated from the Centre Hills volcano between ~0.8 and 0.4 Ma. These dates  
583 extend the period of Centre Hills volcanism to slightly younger ages, and reduce the  
584 apparent gap in subaerial volcanism before the oldest dated activity further south on  
585 Montserrat, at ~290 ka (Harford et al., 2002). Volcaniclastic deposits in submarine  
586 sedimentary sequences provide no evidence of prolonged pauses in volcanism at  
587 Montserrat (Coussens et al., 2016).

### 588 589 3.4 Eruption Parameters

590 Partial isopachs have been constructed for tephra fall deposits (Table 1) that could be  
591 correlated across multiple sites, using maximum cumulative fall deposit thicknesses at each  
592 site (Figure 12). Constraints are generally poor due to limited subaerial exposure. Katy Hill  
593 was assumed as the vent location for all eruptions, and isopach shapes were estimated by  
594 fitting an ellipse to the available data. Isopach width is very poorly constrained for all  
595 deposits. The area of fitted isopachs was used to estimate a minimum fall deposit volume  
596 ( $V_{min}$ ) using  $V_{min} = 3.7 A T$ , where  $A$  is isopach area ( $\text{km}^2$ ) and  $T$  is isopach thickness (m)  
597 (cf. Pyle, 1999). Calculated volumes range between  $0.02 \text{ km}^3$  for the Attic pumice fall  
598 deposits and  $0.43 \text{ km}^3$  for the Woodlands Bay fall deposits (Table 6). Legros et al. (2000)  
599 show that 70% of results are underestimated by at least a factor of two using this method,

600 due to an absence of more distal depositional data. Several of these eruptions, as shown in  
601 Figure 12, also produced thick PDC deposits, with thicknesses exceeding 10 m in some  
602 cases at distances of several kilometres from the vent. The PDC deposit components of  
603 some of these eruptions may be greater in volume than the fall deposit components. Given  
604 these uncertainties, it seems likely that several of these eruptions had total tephra volumes  
605 of up to 0.5 km<sup>3</sup> and that some, such as the Woodlands Bay pumice, were likely >1 km<sup>3</sup>.  
606 Many of these eruptions thus had likely explosive eruption magnitudes of 4–5 (cf. Pyle,  
607 2000).

608

#### 609 **4. Discussion**

##### 610 4.1 History of eruptive activity at Montserrat since 1 Ma

611 Based on the stratigraphy described above and on previous studies of Soufrière Hills (e.g.,  
612 Roobol and Smith 1998; Harford et al., 2002; Smith et al., 2007) we have divided volcanic  
613 activity on Montserrat since 1 Ma into six episodes (Figure 13). Divisions between these  
614 episodes mark an absence of subaerial eruption related products, a change in eruptive vent,  
615 or a change in dominant eruptive style. The oldest unit identified here (South Lime Kiln  
616 Bay pumice) is not included in this summary because it could not be correlated with the  
617 rest of the stratigraphy and may originate from Silver Hills, or from the transitional period  
618 between the end of volcanic activity at Silver Hills and the onset of Centre Hills volcanism.

619

##### 620 *Centre Hills Episode 1, >0.95 to ~0.6 Ma*

621 The oldest dated unit from Centre Hills is andesitic lava from an old lava-dome complex at  
622 the southern edge of Centre Hills, dated at 0.95 Ma (Harford et al., 2002). The major part  
623 of the stratigraphic sequence identified here forms a sequence of lithic breccias interbedded  
624 with pumiceous deposits from sustained explosive eruptions, erupted between ~0.8 and  
625 ~0.6 Ma. Deposits from this period are exposed northeast of Centre Hills and more  
626 extensively to the west and southwest of Centre Hills. There are no internal divisions that  
627 can be used to break this period up further. Since the base of these deposits (or a  
628 recognisable transition to Silver Hills deposits) is not exposed, we define the start of this  
629 first stage of Centre Hills volcanism at >0.95 Ma. The period included at least eight large  
630 explosive eruptions (and additional smaller, uncorrelated deposits), producing andesitic  
631 pumiceous deposits (with the exception of the Angry Bird basaltic andesite), and frequent  
632 effusive eruptions of compositionally similar andesitic lava (cf. Harford et al., 2002;  
633 Zellmer et al., 2003), whose collapse and erosion has generated extensive lithic breccias  
634 around the flanks of Centre Hills. The production of large explosive eruptions of evolved  
635 magma suggests a mature volcanic system. Active vent sites may have existed during this  
636 period to the south of the currently exposed Centre Hills rocks, given the wide eroded  
637 submarine shelf around Bransby Point (similar in width to the shelf around Centre Hills),  
638 and the distributional pattern of some tephra fall deposits (e.g. Bransby Point pumice).

639

##### 640 *Centre Hills Episode 2, ~0.6 to ~0.4 Ma*

641 We have defined a second period of Centre Hills volcanism, based on our interpretation of  
642 the subaerial volcanic stratigraphy, where the three youngest pumiceous deposits (Bunkum  
643 Bay, Woodlands Bay and Attic pumices) are preserved as thick PDC deposits at sites lying  
644 slightly further north than the older units, and are well exposed west and northwest of  
645 Centre Hills. It is unclear from the dating if there was a prolonged (10<sup>5</sup> year) gap in  
646 explosive volcanism, but the distribution of these units suggests a more northerly vent,  
647 consistent with the current peak of the Centre Hills volcano at Katy Hill. As in Episode 1,  
648 this stage of volcanism involved sustained explosive eruptions, including the largest-

649 volume explosive eruption deposit on Montserrat, the Woodlands Bay pumice, interspersed  
650 with effusive andesitic lava-dome forming eruptions.

651

652 Although the vent site may have moved to a more northerly position, both Episodes 1 and  
653 2 at Centre Hills are characterised by effusive and large explosive eruptions throughout the  
654 history of the volcano, without any apparent transitions in dominant eruptive behaviour.

655 However, the youngest explosive eruption deposit, the Attic pumice, is distinctive. Its  
656 dacitic composition is more evolved than any other known volcanic rocks on Montserrat.  
657 The deposit forms the uppermost part of the stratigraphy west of Centre Hills, and is well  
658 exposed in road cuttings, where it lies immediately beneath the soil surface. It may  
659 potentially mark the final eruption of the Centre Hills volcano, and it is thus notable that  
660 this final event is compositionally distinctive, representing a maturation of the system  
661 towards more silica-rich compositions (and with stable amphibole in the phase assemblage,  
662 unlike any preceding Centre Hills eruptions).

663

664 *Soufrière Hills Episode 1, >0.3 to 0.175 Ma*

665 After the Attic pumice eruption, the next identified volcanism on Montserrat moved to the  
666 south, potentially distributed between effusive vents west of Soufrière Hills, around  
667 Garibaldi, Richmond and St Georges Hills (cf. Harford et al., 2002; Smith, 2007). It is  
668 uncertain if both the Soufrière and Centre Hills systems were active at the same time, but  
669 there is no prolonged gap in volcanoclastic deposition in the offshore stratigraphy at this  
670 time (Coussens et al., 2016). Onshore, this period of volcanism on southern Montserrat is  
671 poorly exposed.

672

673 *Soufrière Hills Episode 2, 0.175 to 0.13 Ma*

674 Several lava domes from this period have been dated around Soufrière Hills, and the period  
675 is characterised by andesitic effusive volcanism and small- to moderate-sized explosive  
676 eruptions, preserved as pumiceous lapilli and tuff fall deposits up to 1.5 m thick and  
677 pumiceous surge deposits up to 2 m thick to the south of Soufrière Hills (Roobol and Smith,  
678 1998; Smith, 2007). These deposits are the only evidence of sustained explosive eruptions  
679 from Soufrière Hills. The predominantly effusive andesitic behaviour of Soufrière Hills is  
680 thus in sharp contrast to the Centre Hills stratigraphy described here, which produced large  
681 explosive eruptions, alongside effusive activity, throughout its history.

682

683 *South Soufrière Hills Episode, ~0.13 Ma*

684 At ~0.13 Ma activity at Soufrière Hills shifted onto the south flank of the edifice, forming  
685 the South Soufrière Hills. This eruption produced basaltic scoria deposits with interleaving  
686 basaltic lava flows and andesite lithic breccias, which are more mafic than any other  
687 volcanic rocks from Montserrat (Smith, 2007; Cassidy et al., 2014b, 2015).

688

689 *Soufrière Hills Episode 3, <112 ka*

690 Activity at Soufrière Hills returned to the central vent site after the South Soufrière Hills  
691 episode (Harford et al., 2002), and has been dominated by effusive eruptions of andesitic  
692 lava domes throughout this period, interspersed with short-lived vulcanian explosive pulses,  
693 and generating extensive andesite lithic breccias around the volcano (Wadge and Isaacs,  
694 1988; Roobol and Smith, 1998; Smith et al., 2007). Lavas erupted in this episode at  
695 hornblende-hypersthene andesites, in contrast with the clinopyroxene-hypersthene  
696 andesites that erupted in Episode 2 and throughout the history of Centre Hills (with the  
697 exception of the Attic pumice).

698

699 4.2 Comparison between Centre Hills and Soufrière Hills

700 The stratigraphy of the Soufrière Hills complex differs markedly from the stratigraphy of  
701 Centre Hills. Thick (>1 m) pumiceous deposits from sustained explosive eruptions are  
702 present throughout the stratigraphy of Centre Hills, but are confined to the early stages of  
703 activity at Soufrière Hills (Episode 2), and even at this time do not appear to have been as  
704 large or frequent (based on their limited preservation) as those from Centre Hills.

705

706 Rocks from Soufrière Hills Episode 3, and particularly those from the most recent eruption,  
707 have been far more extensively studied (e.g., Barclay et al., 1998; Edmonds et al., 2001;  
708 Devine et al., 2003; Humphreys et al., 2009) than older rocks from both Soufrière Hills and  
709 Centre Hills (e.g., Zellmer et al., 2003; Devine et al., 2003; Cassidy et al., 2015). However,  
710 available data suggests that, throughout the history of the two volcanoes, effusive eruptions  
711 have involved similar styles (dome extrusion and generation of associated lithic breccia  
712 deposits) and have erupted products of similar mineralogy and chemistry. No long-term  
713 chemical trends have characterised this period, but there is evidence of periodic short-lived  
714 departures to the eruption of different magma compositions (e.g. the basaltic andesite  
715 Angry Bird pumice (and the lava flow directly beneath it; an unusual style of effusive  
716 activity on Montserrat) in the earliest stages of Centre Hills, the dacitic Attic pumice at the  
717 end of Centre Hills, and the South Soufrière Hills episode). These departures mark  
718 transitions in the magma system, occurring near the start and at the end of Centre Hills  
719 activity, and marking a shift in stable phase assemblage at Soufrière Hills each side of the  
720 South Soufrière Hills episode.

721

722 The clinopyroxene-hypersthene andesites at Centre Hills are very similar in bulk  
723 composition to those from both Soufrière Hills Episodes 2 and 3, and petrographically  
724 similar to those from Episode 2. Incompatible trace element patterns for both volcanoes  
725 have comparable trough-shaped patterns related to MREE removal by amphibole  
726 crystallisation (Figure 14), supporting an interpretation of comparable magma-genetic  
727 processes between the two systems (cf. Cassidy et al., 2012). The eruption of hypersthene-  
728 hornblende andesites in Soufrière Hills Episode 3 was not associated with a change in bulk  
729 compositions. The only comparable transition at Centre Hills occurs in the youngest  
730 eruption at the volcano (the Attic pumice), and is associated with a change in bulk  
731 chemistry to more silicic compositions. The presence of amphibole in the Attic pumice  
732 may reflect cooling of the magma reservoir, promoting amphibole stability (hornblende  
733 becomes unstable at >880 °C at upper crustal pressures in Montserrat's andesite magmas  
734 (Barclay et al., 1998; Devine et al., 2003)). Our limited number of estimated magma  
735 storage temperatures for Centre Hills suggests higher temperatures for magmas feeding  
736 explosive eruptions at Centre Hills (900-1000° C) than those estimated for the recent  
737 Soufrière Hills eruption (based on Fe-Ti oxide temperature estimates of ~870° C;  
738 Christopher et al., 2014), and it is possible that there is a temperature related control on  
739 both the stable phenocryst assemblage and the dominant eruptive style on Montserrat,  
740 although this interpretation requires further investigation.

741

742 The youngest (<24 ka; older units have not been studied) products of Soufrière Hills show  
743 a notable difference in the abundance and composition of enclaves when compared with  
744 the Centre Hills explosive eruption deposits. At Soufrière Hills, mafic enclaves occur  
745 within lithic and pumice clasts and make up 1–12 vol.% of recent (1995-2010) eruptive  
746 products (Plail et al., 2014). These enclaves are interpreted as evidence of late-stage  
747 intrusion of mafic magma into the upper crustal storage region, resulting in mingling and  
748 localised heating (Barclay et al., 1998; Humphreys et al., 2009). Within the Centre Hills

749 units we found no evidence of this process and no mafic enclaves; all enclaves in the  
750 pumices are andesitic, with a similar mineralogy to the rest of Centre Hills deposits,  
751 suggesting that a different process was driving the large explosive eruptions at Centre Hills.  
752 Although large explosive eruptions occurred throughout the Centre Hills period, effusive,  
753 lava-dome forming eruptions occurred alongside these, and lithic deposits from these  
754 eruptions comprise the bulk of the exposed stratigraphy around Centre Hills. A number of  
755 factors influence the explosivity of eruptions, including melt composition, gas content,  
756 magma viscosity, temperature, and vent and conduit geometries (Wilson et al., 1980;  
757 Scandone et al., 2007; Koleszar et al., 2012; Nguyen et al., 2014). Identifying a particular  
758 cause of the difference in behaviour between the two volcanoes is therefore difficult,  
759 although the dominant magma composition has been constant on Montserrat throughout  
760 the past million years, suggesting that magma composition is not the driver of changes in  
761 eruption style. Explosive eruptions are observed throughout the history of Centre Hills,  
762 even through periods of possible migration of the vent site, and there is no evidence to  
763 suggest that the dominant style of eruption is related to the maturity of the magma system  
764 or the size of the overlying edifice (e.g., Pinel and Jaupart, 2000; Taisne and Jaupart, 2008).  
765 The difference in enclave content, noted above, may mark a significant difference in the  
766 typical eruption triggering process, and our observations of hornblende stability and  
767 limited thermometry suggest that the current Soufrière Hills system may be cooler than the  
768 Centre Hills system. It is possible that temperature-related differences in viscosity and  
769 ascent behaviour enabled explosive eruption styles at Centre Hills, but this inference  
770 remains speculative.

771

## 772 **5. Conclusions**

773 This study substantially extends the stratigraphic record of volcanic activity on Montserrat,  
774 identifying several distinct episodes of volcanism since 1 Ma, characterised by shifts in  
775 vent site or dominant eruption style. We identify 11 thick (>1 m) pumiceous units (and a  
776 similar number of less well exposed units) derived from sustained explosive eruptions of  
777 the Centre Hills volcano, some of which have likely tephra volumes of >1 km<sup>3</sup> (e.g.,  
778 Woodlands Bay pumice). The presence of multiple pumiceous deposits, interbedded with  
779 lithic breccias derived from effusive eruptions, implies that there were repeated sustained  
780 explosive eruptions throughout the lifetime of Centre Hills, alongside effusive, lava-dome  
781 forming eruptions. The volcanic rocks erupted throughout this period are andesites with  
782 very similar bulk chemical and mineralogical compositions. The final explosive eruption of  
783 Centre Hills, that Attic pumice, departs from this pattern and has a dacitic composition.

784

785 Following the Attic pumice eruption, activity moved southwards to the Soufrière Hills  
786 volcano. The earlier stages of Soufrière Hills activity erupted andesites of very similar  
787 composition to the Centre Hills rocks, with evidence of some sustained explosive activity  
788 alongside more common effusive eruptions. Following the basaltic South Soufrière Hills  
789 episode at ~130 ka, activity at Soufrière Hills switched to predominantly effusive activity,  
790 without large explosive eruptions. The magma erupted in this final episode has identical  
791 bulk compositions to preceding andesitic activity, but has a hypersthene-hornblende  
792 phenocryst assemblage, in contrast to the clinopyroxene-hypersthene assemblage that  
793 characterises earlier episodes of andesitic volcanism on Montserrat.

794

795 The notably greater propensity towards explosive volcanism at Centre Hills contrasts with  
796 a marked absence of similar activity at Soufrière Hills, especially since ~130 ka. An  
797 additional difference is the common occurrence of mafic enclaves in the Soufrière Hills  
798 rocks, which are absent in the pumiceous deposits from Centre Hills. The bulk composition

799 of the erupted andesite has remained very similar on Montserrat since 1 Ma. This  
800 compositional stability suggests that local changes in magma storage conditions  
801 (potentially causing small differences in magma temperature or viscosity) and pre-eruptive  
802 dynamics, rather than shifts in magma composition, are the major control on eruption style  
803 during prolonged ( $10^5$  year timescales) episodes of volcanism on Montserrat.

804

## 805 **6. Acknowledgments**

806 We thank the Montserrat Volcano Observatory for support during fieldwork, and Paul Cole,  
807 Eliza Calder, Ben Edwards, Rod Stewart and Adam Stinton for advice on field sites. Ar-Ar  
808 dates were funded by the NERC Isotope Geosciences Facility allocation IP-1401-1113. We  
809 thank Jim Imlach for assistance in sample preparation and dating, and Agnes Michalik,  
810 Ben Buse, Stuart Kearns and Ian Croudace for assistance with geochemical analyses. We  
811 acknowledge funding from NERC grants NE/K000403/1 and NE/I02044X/1 (SW) and  
812 Humboldt fellowship (MC).

813

## 814 **7. References**

- 815 Bacon, C.R., Lanphere, M.A., 2006. Eruptive history and geochronology of Mount  
816 Mazama and the Crater Lake region, Oregon. Geological Society of America  
817 Bulletin 118, 1331-1359.
- 818 Baker, P.E., 1985. Volcanic hazards on St Kitts and Montserrat, West Indies. Journal of the  
819 Geological Society of London 142, 279-295.
- 820 Barclay, J., Rutherford, M.J., Carroll, M.R., 1998. Experimental phase equilibria constraints  
821 on pre-eruptive storage conditions of the Soufrière Hills magma. Geophysical  
822 Research Letters 25, 3437-3440.
- 823 Branney, M.J., Kokelaar, B.P., 2002. Pyroclastic density currents and the sedimentation of  
824 ignimbrites. Geological Society, London, Memoirs, 27.
- 825 Brown, K., Davidson, C., 2008.  $^{40}\text{Ar}/^{39}\text{Ar}$  geochronology of the Silver Hills andesite,  
826 Montserrat, West Indies. B.A. Senior Integrative Exercise, Carleton College,  
827 Northfield, Minnesota.
- 828 Brown, R.J., Civetta, L., Arienzo, I., D'Antonio, M., Moretti, R., Orsi, G., Tomlinson, E.  
829 L., Albert, P.G., Menzies, M.A., 2014. Geochemical and isotopic insights into the  
830 assembly, evolution and disruption of a magmatic plumbing system before and after  
831 a cataclysmic caldera-collapse eruption at Ischia volcano (Italy). Contributions to  
832 Mineralogy and Petrology 168, 1-23.
- 833 Cassidy, M., Taylor, R.N., Palmer, M.R., Cooper, R.J., Stenlake, C., Trofimovs, J., 2012.  
834 Tracking the magmatic evolution of island arc volcanism: Insights from a high-  
835 precision Pb isotope record of Montserrat, Lesser Antilles. Geology, Geochemistry,  
836 Geophysics 13, 1525-2027.
- 837 Cassidy, M., Watt, S.F.L., Palmer, M.R., Trofimovs, J., Symons, W., Maclachlan, S.E.,  
838 Stinton, A.J., 2014a. Construction of volcanic records from marine sediment cores: A  
839 review and case study (Montserrat, West Indies). Earth-Science Reviews 138, 137-  
840 155.
- 841 Cassidy, M., Trofimovs, J., Watt, S.F.L., Palmer, M.R., Taylor, R.N., Gernon, T.M.,  
842 Talling, P.J., Le Friant, A., 2014b. Multi-stage collapse events in the South Soufrière  
843 Hills, Montserrat, as recorded in marine sediment cores. Geological Society,  
844 Memoirs, 39, 383-397.
- 845 Cassidy, M., Watt, S.F.L., Talling, P.J., Palmer, M.R., Edmonds, M., Jutzeler, M., Wall-  
846 Palmer, D., Manga, M., Coussens, M., Gernon, T., Taylor, R.N., Michalik, A., Inglis,  
847 E., Bretkreuz, C., Le Friant, A., Ishizuka, O., Boudon, G., McCanta, M.C., Adachi,  
848 T., Hornbach, M.J., Colas, S.L., Endo, D., Fujinawa, A., Kataoka, K.S., Maeno, F.,

849 Tamura, Y., Wang, F., 2015, Rapid onset of mafic magmatism facilitated by volcanic  
850 edifice collapse. *Geophysical Research Letters* 42, 4778-4785.

851 Christopher, T.E., Humphreys, M.C., Barclay, J., Genareau, K., De Angelis, S.M., Plail,  
852 M., Donovan, A., 2014. Petrological and geochemical variation during the Soufrière  
853 Hills eruption, 1995 to 2010. *Geological Society, Memoirs*, 39, 317-342.

854 Coussens, M.F., Wall-Palmer, D., Talling, P.J., Watt, S.F.L., Cassidy, M., Jutzeler, M.,  
855 Clare, M.A., Hunt, J.E., Manga, M., Gernon, T.M., Palmer, M.R., Hatter, S.J.,  
856 Boudon, G., Endo, D., Fujinawa, A., Hatfield, R., Hornbach, M.J., Ishizuka, O.,  
857 Kataoka, K., Le Friant, A., Maeno, F., McCanta, M., Stinton, A.J., 2016. The  
858 relationship between eruptive activity, flank collapse and sea-level at volcanic  
859 islands: a long-term (>1 Ma) record offshore Montserrat, Lesser Antilles.  
860 *Geochemistry, Geophysics, Geosystems* 17, 2591-2611.

861 Devine, J.D., Rutherford, M.R., Norton, G.E., Young, S.R., 2003. Magma storage region  
862 processes inferred from geochemistry of Fe-Ti oxides in andesitic magma, Soufrière  
863 Hills Volcano, Montserrat, W.I. *Journal of Petrology* 44, 1375-1400.

864 Druitt, T.H., Mellors, R.A., Pyle, D.M., Sparks, R.S.J., 1989. Explosive volcanism on  
865 Santorini, Greece. *Geological Magazine* 126, 95-126.

866 Druitt, T.H., Kokelaar, B.P., 2002. The eruption of Soufrière Hills Volcano, Montserrat,  
867 from 1995 to 1999. *Geological Society, London, Memoirs*, 21.

868 Edmonds, M., Pyle, D., Oppenheimer, C., 2001. A model for degassing at the Soufrière  
869 Hills Volcano, Montserrat, West Indies, based on geochemical evidence. *Earth and  
870 Planetary Science Letters* 186, 159-173.

871 Germa, A., Quidelleur, X., Lahitte, P., Labanieh, S., Chauvel, C., 2011. The K-Ar  
872 Cassinot-Gillot technique applied to western Martinique lavas: A record of Lesser  
873 Antilles arc activity from 2 Ma to Mount Pelée volcanism. *Quaternary Geology* 6,  
874 341-355.

875 Harford, C.L., Pringle, M.S., Sparks, R.S.J., Young, S.R., 2002. The volcanic evolution of  
876 Montserrat using  $^{40}\text{Ar}/^{39}\text{Ar}$  geochronology. *Geological Society, Memoirs*, 21, 93-  
877 113.

878 Humphreys, M.C.S., Blundy, J.D., Sparks, R.S.J., 2006. Magma evolution and open-  
879 system processes at Shiveluch volcano: insights from phenocryst zoning. *Journal of  
880 Petrology* 47, 2303-2334.

881 Humphreys, M.C.S., Christopher, T., Hards, V., 2009. Microlite transfer by disaggregation  
882 of mafic inclusions following magma mixing at Soufrière Hills volcano, Montserrat.  
883 *Contributions to Mineralogy and Petrology* 157, 609-624.

884 Koleszar, A.M., Kent, A.J.R., Wallace, P.J., Scott, W.E., 2012. Controls on long-term low  
885 explosivity at andesitic arc volcanoes: insights from Mount Hood, Oregon. *Journal of  
886 Volcanology and Geothermal Research* 219-220, 1-14.

887 Legros, F., 2000. Minimum volume of a tephra fallout deposit estimated from a single  
888 isopach. *Journal of Volcanology and Geothermal Research* 96, 25-32.

889 Lowe, D.J., 2011. Tephrochronology and its application: A review. *Quaternary Geology* 6,  
890 107-153.

891 Nguyen, C.T., Gonnermann, H.M., Houghton, B.F., 2014. Explosive to effusive transition  
892 during the largest volcanic eruption of the 20th century (Novarupta 1912, Alaska).  
893 *Geology* 42, 703-706.

894 Pinel, V., Jaupart, C., 2000. The effect of edifice load on magma ascent beneath a volcano.  
895 *Philosophical Transactions of the Royal Society, A* 358, 1515-1532.

896 Plail, M., Barclay, J., Humphreys, M.C.S., Edmonds, M., Herd, R.A., Christopher, T.E.,  
897 2014. Characterization of mafic enclaves in the erupted products of Soufrière Hills  
898 Volcano, Montserrat, 2009 to 2010. *Geological Society, Memoirs* 39, 343-360.

- 899 Putirka, K., Johnson, M., Kinzler, R., Longhi, J., Walker, D., 1996. Thermobarometry of  
900 mafic igneous rocks based on clinopyroxene-liquid equilibria, 0–30 kbar.  
901 Contributions to Mineralogy and Petrology 123, 92-108.
- 902 Putirka, K.D., Mikaelian, H., Ryerson, F., Shaw, H., 2003. New clinopyroxene-liquid  
903 thermobarometers for mafic, evolved, and volatile-bearing lava compositions, with  
904 applications to lavas from Tibet and the Snake River Plain, Idaho. American  
905 Mineralogist 88, 1542-1554.
- 906 Putirka, K.D., 2005. Mantle potential temperatures at Hawaii, Iceland, and the mid-ocean  
907 ridge system, as inferred from olivine phenocrysts: evidence for thermally driven  
908 mantle plumes. Geochemistry, Geophysics, Geosystems 6, 5.
- 909 Putirka, K.D., 2008. Thermometers and barometers for volcanic systems. In: Putirka, K.D.,  
910 Tepley, F.J.I. (Eds.), Minerals, Inclusions, and Volcanic Processes. Mineralogical  
911 Society of America, pp. 61-120.
- 912 Pyle, D.M., 1999. Widely dispersed Quaternary tephra in Africa. Global and Planetary  
913 Change 21, 95-112.
- 914 Pyle, D.M., 2000. Sizes of volcanic eruptions. In: Sigurdsson, H., Houghton, B., Rymer,  
915 H., Stix, J., McNutt, S. (Eds.), Encyclopedia of Volcanoes. Academic Press, pp. 263-  
916 269.
- 917 Rea, W.J., 1975. The volcanic geology and petrology of Montserrat, West Indies. Journal  
918 of the Geological Society of London 130, 341-366.
- 919 Ridolfi, F., Renzulli, A., Puerini, M. (2010). Stability and chemical equilibrium of  
920 amphibole in calc-alkaline magmas: an overview, new thermobarometric  
921 formulations and application to subduction-related volcanoes. Contributions to  
922 Mineralogy and Petrology 160, 45-66.
- 923 Roobol, M.J., Smith, A.L., 1998. Pyroclastic stratigraphy of the Soufrière Hills volcano,  
924 Montserrat - implications for the present eruption. Geophysical Research Letters 25,  
925 3393-3396.
- 926 Scandone, R., Cashman, K.V., Malone, S.D., 2007. Magma supply, magma ascent and the  
927 style of volcanic eruptions. Earth and Planetary Science Letters 253, 513-529.
- 928 Singer, B.S., Jicha, B.R., Harper, M.A., Naranjo, J.A., Lara, L.E., Moreno-Roa, H., 2008.  
929 Eruptive history, geochronology, and magmatic evolution of the Puyehue-Cordón  
930 Caulle volcanic complex, Chile. Geological Society of America Bulletin 120, 599-  
931 618.
- 932 Smith, A.L., 2007. Prehistoric stratigraphy of the Soufrière Hills-South Soufrière Hills  
933 volcanic complex, Montserrat, West Indies. The Journal of Geology 115, 115-127.
- 934 Taisne, B., Jaupart, C., 2008. Magma degassing and intermittent lava dome growth.  
935 Geophysical Research Letters 35, L20310.
- 936 Trofimovs, J., Talling, P.J., Fisher, J.K., Hart, M.B., Sparks, R.S.J., Watt, S.F.L., Cassidy,  
937 M., Smart, C.W., Le Friant, A., Moreton S.G., Lang, M.J., 2013. Timing, origin and  
938 emplacement dynamics of mass flows offshore of SE Montserrat in the last 110 ka:  
939 Implications for landslide and tsunami hazards, eruption history, and volcanic island  
940 evolution. Geochemistry, Geophysics, Geosystems 14, 385-406.
- 941 Wadge, G., Isaacs, M.C., 1988. Mapping the volcanic hazards from Soufrière Hills volcano,  
942 Montserrat, West Indies using an image processor. Journal of the Geological Society  
943 145, 541-551.
- 944 Wadge, G., Voight, B., Sparks, R.S.J., Cole, P.D., Loughlin, S.C., Robertson, R.E.A., 2014.  
945 An overview of the eruption of Soufrière Hills Volcano, Montserrat from 2000 to  
946 2010. Geological Society, Memoirs, 39, 1-39.
- 947 Watt, S.F.L., Talling, P.J., Vardy, M.E., Masson, D.G., Henstock, T.J., Hühnerbach, V.,  
948 Minshull, T.A., Urlaub, M., Lebas, E., Le Friant, A., Berndt, C., Crutchley, G.J.,

949 Karstens, J., 2012. Widespread and progressive seafloor-sediment failure following  
950 volcanic debris avalanche emplacement: Landslide dynamics and timing offshore  
951 Montserrat, Lesser Antilles. *Marine Geology* 323-325, 69-94.  
952 White, J.D.L., Houghton, B.F., 2006. Primary volcanoclastic rocks. *Geology* 34, 677-680.  
953 Wilson, L., Sparks, R.S.J., Walker, G.P.L., 1980. Explosive volcanic eruptions—IV. The  
954 control of magma properties and conduit geometry on eruption column behaviour.  
955 *Geophysical Journal of the Royal Astronomical Society* 63, 117-148.  
956 Zellmer, G.F., Hawkesworth, C.J., Sparks, R.S.J., Thomas, L.E., Harford, C.L., Brewer,  
957 T.S., Loughlin, S.C., 2003. Geochemical evolution of the Soufrière Hills volcano,  
958 Montserrat, Lesser Antilles volcanic arc. *Journal of Petrology* 44, 1349-1374.  
959

## 960 **8. Supplementary Information**

961 Supplementary Figure 1: High resolution stratigraphic logs of the Centre Hills units.  
962 Supplementary Table 1: List of all analysed samples with site locations  
963 Supplementary Table 2: Complete XRF analyses for all analysed samples  
964 Supplementary Table 3: Complete ICP-MS analyses for all analysed samples.  
965 Supplementary Table 4: Plagioclase composition and precision data from SEM analysis  
966 Supplementary Table 5: Clinopyroxene composition and precision data from SEM analysis  
967 Supplementary Table 6: Orthopyroxene composition and precision data from SEM analysis  
968 Supplementary Table 7: Amphibole composition and precision data from SEM analysis  
969 Supplementary Table 8: Glass compositions from EMP analysis  
970 Supplementary Table 9: Standard Deviation of glass compositions from EMP analysis.  
971

## 972 **Figure Captions**

973 **Figure 1:** Map of Montserrat showing the volcanic centres and selected geographic  
974 locations. All field sites are shown as circles, with the numbers indicating the location of  
975 specific samples, named in the key and shown in stratigraphic context in Figures 2 and 3.  
976

977 **Figure 2:** Summary stratigraphic logs for sites west of Centre Hills (the most northerly site  
978 is at the left of the figure). Clast types and their relative concentration and sorting are  
979 shown schematically within each unit. Pumiceous deposits are identified as coloured bands.  
980 In many cases deposits form discontinuous horizons, and their correlation between sites  
981 has been based on physical characteristics (appearance, grain size, internal structure and  
982 stratigraphic order), confirmed in some cases by chemical analysis. Pumiceous units are  
983 separated by undifferentiated sequences of lithic breccias. Stratigraphic positions of  
984 samples (and the type of analysis, where relevant) are indicated. Full location details for all  
985 samples are provided as Supplementary Data.  
986

987 **Figure 3:** Summary stratigraphic logs for sites east of Centre Hills (the most northerly site  
988 is at the left of the figure). Clast types and their relative concentration and sorting are  
989 shown schematically within each unit. Pumiceous deposits are identified as coloured bands.  
990 In many cases deposits form discontinuous horizons, and their correlation between sites  
991 has been based on physical characteristics (appearance, grain size, internal structure and  
992 stratigraphic order), confirmed in some cases by chemical analysis. Pumiceous units are  
993 separated by undifferentiated sequences of lithic breccias. Stratigraphic positions of  
994 samples (and the type of analysis, where relevant) are indicated. Full location details for all  
995 samples are provided as Supplementary Data.  
996

997 **Figure 4:** Photographs of selected exposure of the pumice-rich units described here. Photo  
998 locations (latitude and longitude) and unit names are shown beneath each image. The tape

999 measure, where shown, is extended to 1 m. The images show characteristic overall unit  
1000 structures (e.g. Woodlands Bay image) or internal detail (e.g. pelletal lapilli in Attic  
1001 Pumice), as well as the nature of the typical bounding stratigraphy for exposures  
1002 throughout the study area (e.g. lithic breccias in Bransby Point and Angry Bird images).

1003  
1004 **Figure 5:** Whole rock major element compositions plotted against silica for pumiceous  
1005 units from central Montserrat. Most units have similar compositions and plot along a single  
1006 fractional crystallisation trend. Nearly all units lie within the andesitic compositional field  
1007 (bottom right) that typifies most volcanic rocks on Montserrat. The Attic pumice is more  
1008 evolved, while the Angry Bird pumice is more mafic (although alteration may have  
1009 affected the bulk chemistry of this unit).

1010  
1011 **Figure 6:** Comparisons of a range of bulk-rock trace (upper panel) and major (lower panel)  
1012 element concentrations against relative stratigraphic age (summarised on the right of each  
1013 panel). All samples except the South Lime Kiln Bay pumice are of Centre-Hills age.  
1014 Compositions are stable throughout the period represented, with the exception of the  
1015 Angry Bird pumice and the slightly more evolved Attic pumice, which is the youngest  
1016 recognised eruption from Centre Hills. There are subtle long term trends towards HREE  
1017 depletion and HFSE enrichment (e.g. Th) in the youngest units.

1018  
1019 **Figure 7:** Nd against Y for whole-rock trace element analyses of pumice for pyroclastic  
1020 units in central Montserrat. These elements allow several individual units to be  
1021 discriminated on the basis of bulk chemistry, defining tight compositional clusters for  
1022 several deposits (e.g. Garibaldi Hill and Old Road Bay pumices).

1023  
1024 **Figure 8:** Ba/La and Th/La for volcanic systems on Montserrat (adapted from Cassidy et  
1025 al., 2012). The basaltic South Soufrière Hills lies in a separate compositional field, and  
1026 Soufrière Hills rocks have slightly higher Ba/La values than those from Centre Hills and  
1027 Silver Hills, which lie in the same compositional field. Samples from this study all lie on  
1028 the Centre and Silver Hills trend, but at slightly higher Th/La values.

1029  
1030 **Figure 9:** Major element analyses of pyroxene phenocryst compositions from pumices in  
1031 selected Centre Hills deposits. Panel A shows the the pyroxene phenocryst composition is  
1032 very similar across all these units (rim and core compositions were highly similar and are  
1033 not differentiated in this figure; full data are provided as Supplementary Tables). Panel B  
1034 shows Al and Fe compositions in the rims of clinopyroxene phenocrysts, indicating that  
1035 subtle variations exist between some units and could potentially be used as a correlative  
1036 tool.

1037  
1038 **Figure 10:** Major element glass composition for pumices from pyroclastic units in central  
1039 Montserrat. For several units pumices were analysed from multiple field sites (e.g. Attic  
1040 and Garibaldi Hill pumices), and the similarity in glass composition between these sites  
1041 supports their correlation. Although there is substantial overlap in glass composition for  
1042 several units, reflecting their very similar bulk-rock chemistry, discrete fields can be  
1043 defined for some deposits (e.g. Foxes and Bunkum Bay pumices). These units could  
1044 potentially be used as marker beds for wider correlation between the subaerial and marine  
1045 stratigraphy around Montserrat.

1046  
1047 **Figure 11:**  $^{40}\text{Ar}/^{39}\text{Ar}$  plateau ages plotted against cumulative percentage of Ar released for  
1048 plagioclase phenocrysts separated from pumices in six of the pyroclastic units studied here.

1049 Dashed lines show mean apparent age and solid lines show errors to  $2\sigma$  at successive steps.  
1050 The age obtained is shown at the top of each panel.

1051

1052 **Figure 12:** Approximate isopach sections constructed for the cumulative thickness of fall  
1053 deposits within the more widely exposed pumiceous units identified from Centre Hills.

1054 Fall unit thicknesses used in constructing isopachs are shown in black text with location  
1055 shown by green circles. Selected flow deposit thicknesses at the same sites are shown in  
1056 red, with flow directions (based on the broad location of the assumed vent site) shown by  
1057 red arrows. In the absence of other information, the vent site is assumed to be located at  
1058 Katy Hill, although as discussed in the text, a more southerly vent site may have been the  
1059 source of the older units described here, and is more consistent with the outcrop patterns  
1060 of units such as the Bransby Point and Garibaldi Hill pumices.

1061

1062 **Figure 13:** A summary of the onshore stratigraphy of Montserrat over the past one million  
1063 years, defining six episodes of volcanism separated by changes in vent site or eruptive  
1064 behaviour. Schematic stratigraphic logs of representative subaerial sequences are shown  
1065 for each episode (scales are approximate and are primarily representative of deposits found  
1066 at the distal margins of the subaerial edifices). The top panel compares the episodes  
1067 defined here with those defined in previous studies by Smith (2007) and Trofimovs et al.  
1068 (2013).

1069 **Figure 14:** Rare Earth element profiles showing the compositional range of analysed rocks  
1070 from Centre Hills, Soufrière Hills and the South Soufrière Hills basaltic episode, adapted  
1071 from Zellmer et al. (2003). Centre Hills rocks overlap entirely with those from Soufrière  
1072 Hills, but show a broader compositional range.

**Table 1: Summary descriptions and interpretation of major pumice-rich deposits in central Montserrat**

| Unit                        | Extent of exposures  | Type locality (latitude; longitude) | Unit samples                              | Sub-unit | Sub-unit lithofacies                       | Thickness, structure, grading           | Lithological description   | Interpretation of depositional process  |
|-----------------------------|--|-------------------------------------|---|----------|--|---|--|---|
| <i>West of Centre Hills</i> |  |                                     |   |          |  |   |  |   |
| Attic Pumice                | Laterally continuous along several road cuttings W of Centre Hills   | N16.75413; E62.22226                | 8.1.1A, 3.3.1G, 3.2.1I+E, 3.2.1F, 3.1.8C  | Upper    | Cross-bedded tuff                          | 1.2 m, massive, with cross-bedded base. | Moderately sorted deposit dominated by subangular-subrounded pumice (90 vol.%) and ash-coated pelletal grains. Maximum pumice size 1 cm; lithics up to 3 cm. Lower part of the subunit contains fewer larger clasts (coarse-tail reverse sorting).   | Primary deposit of low concentration PDC (presence of sedimentary structures; pelletal grains; homogeneous composition).  |
|                             |  |                                     |   | Middle   | Tuff                                       | 2 m, massive                            | Well-sorted, contains >90 vol.% of 2 mm pumices and ash-coated clasts.   | Primary deposit of wet (pelletal grains) tephra fall or possible low-moderate concentration PDC (well sorted, but without sedimentary structures).  |
|                             |  |                                     |   | Lower    | Massive lapilli-tuff                       | 3 m, dm-bedded                          | Moderately to poorly sorted. Variable amounts of pumices, lithics, pelletal grains, and ash. Clasts chiefly 2-5 mm in size. Contains single-clast-thick pumice horizons. Fewer pelletal grains at the base of the sub-unit.  | Primary deposit of moderate concentration PDC (some bedding structures developed).  |
| Woodlands Bay Pumice        | Laterally continuous, can be traced along coastal cliffs on the west coast with individual exposures over ~500 m | N6.76298; E62.22343                 | 5.1.1C, 5.1.1A, 5.1.1B, 10.1.1A, 3.1.2A+B | Upper    | Banded lapilli-tuff                        | 5 m, dm-bedded                          | Moderately sorted, angular lapilli. Comprises >95 vol.% pumices (4.5 cm mean size, max clast size 18 cm), and <5 vol.% grey lithics (max 5 cm). Very little (<1 vol.%) finer-grained matrix.   | Primary tephra fall (moderately well sorted, consistent thickness, angular clasts, pumice dominated).   |
|                             |  |                                     |   | Middle   | Interbedded lapilli-tuff                   | 7 m, dm-m bedded                        | A sequence of decimetre pumice lapilli beds defined by ash-rich and ash-poor alternating beds. Ash rich beds: poor to moderately sorted, subangular, <40 vol.% ash matrix, 10-20 vol.% lithics, and up to 60 vol.% pumice lapilli, mean size 1 cm. Contains pumice lapilli lenses and single-clast-thick pumice horizons. Pumice rich: Moderately sorted, angular. Comprises 70-90 vol.% pumices, 30 vol.% lithics, and 10 vol.% ash. Pumice mean size 2-4 cm, max 11 cm.              | Primary tephra fall deposits (lapilli beds) interleaved with moderately concentrated PDC deposits (poor-moderate sorting; relatively high ash content). Some fall deposits may be reworked at the top by subsequent PDCs. |
|                             |  |                                     |   | Lower    | Lapilli-tuff                               | 4.5 m, dm-m bedded                      | Variably sorted, angular-subangular lapilli deposit, with wide variation in pumice lapilli content (20-90 vol.%), ash content (10-90 vol.%) and lithic content (10-50 vol.% ) between individual beds. Mean clast size 1-2cm. Occasional well sorted pumice lapilli lenses.  | Deposit from high concentration PDCs, potentially with partial reworking.   |
| Bunkum Bay Pumice           | Crops out in isolated lenses (<50 m laterally), often as channelised sequences                                   | N16.77193; E62.22037                | 6.1.4B, 6.1.2A, 3.4.2H                    | Upper    | Lapilli-tuff                               | 7 m, massive, discordant basal contact. | Poorly-sorted, polymict deposit of pumice and lithic clasts. Detailed composition uncertain due to inaccessible outcrop.   | Possibly reworked (e.g. laharcic) deposit derived from underlying deposit.  |
|                             |  |                                     |   | Lower    | Interbedded lapilli-tuff and tuff channels | 0-7m, channel deposits.                 | Alternating units of tuff and lapilli-tuff. Tuff units: moderate-well sorted, laminated with accretionary lapilli-rich (3mm) and pumice-rich horizons (up to 2 cm in size) in a matrix of orange medium-grained ash with 20 vol.% plagioclase and pyroxene crystals. Lapilli-tuff horizons: Poorly-sorted, angular. Comprises 65-90 vol.% pumices (5 cm maximum size), 5-15 vol.% grey and altered lithics, and <5-20 vol.% coarse grey ash rich in plagioclase and pyroxene crystals. | Primary deposits of alternating high and low concentration phases of PDCs (alternation between well-sorted, laminated deposits to poorly-sorted deposits). Accretionary lapilli suggest wet environment.                  |
| Foxes Pumice                | Crops out in one isolated  | N16.72365; E62.24035                | 4.2.5I, 4.2.2E                            | Upper    | lapilli-tuff                               | 3 m, massive to dm-bedded.              | Well-sorted, angular pumice lapilli (>90 vol.%; 2-5 mm in size) with <10 vol.% ash and <1 vol.% lithics.   | Primary tephra fall (well sorted, dominated by angular pumice).   |

|                            |  |                      |  |        |                              |   |   |   |
|----------------------------|--|----------------------|--|--------|------------------------------|---|---|---|
|                            | cliff section, traceable for ~50 m                                     |                      |  | Lower  | Tuff                         | 20 cm, laminated.                       | Well-sorted pink medium-grained ash.  | Primary tephra fall or possibly low concentration density current.  |
| Old Road Bay Tuff          | Present from Old Road Bay to Lime Kiln Bay, thinning N.                | N16.73722; E62.23302 | 2.1.2B   | Upper  | Bedded lapilli-Tuff          | 1 m, cm-bedded.                         | Well sorted, subangular pumice lapilli within ash matrix, alternating between yellow ash beds and thin pumice horizons (1 cm beds; pumice maximum size 1 cm).   | Primary tephra fall from pulsed eruption or low concentration PDC.  |
|                            |  |                      |  | Lower  | Tuff                         | 50 cm, dm-bedded                        | Well sorted, laminated tuff, laterally continuous. Top and base are grey, middle is yellow  | Primary tephra fall (well sorted, laterally continuous)   |
| Bransby Point Pumice       | Laterally continuous for ~3 km around Bransby Point towards Plymouth   | N16.72365; E62.24035 | BP   | Upper  | Massive lapilli-tuff         | 1 m, massive                            | Well-sorted, angular pumice lapilli, with laterally consistent thickness. Comprises >90 vol.% of pink pumices (max 4.5 cm), 5 vol.% grey lithics (max 2.5 cm), and 5 vol.% pink ash. Some discontinuous 1 cm thick ash horizons within deposit. Capped by a thin (~5 cm) ash layer.   | Primary tephra fall (well sorted angular clasts, pumice rich, laterally continuous).  |
|                            |  |                      |  | Lower  | Massive lapilli-tuff         | 1 m, dm-bedded                          | Well-sorted, angular white pumice lapilli (>95 vol.%; max size 5 cm), 5 vol.% grey lithics, <1 vol.% white fine-medium ash. Capped by a thin (<10 cm) pink ash.   | Primary tephra fall (well sorted angular clasts, pumice rich, laterally continuous).  |
| Garibaldi Hill Pumice      | Laterally continuous, thickening southwards. Tilted at Garibaldi Hill. | N16.72899 E62.23521  | 4.1.4H, 5.2.3E, 11.1.3B, 9.2.1C, 9.2.1D, 7.1.1A  | Upper  | Lapilli-tuff                 | 50 cm, massive.                         | Well-sorted, angular yellow pumice lapilli (95 vol.%; max size 4 cm), 5 vol.% lithics, and <1 vol.% yellow medium-grained ash.  | Primary tephra fall (well sorted angular clasts, pumice rich, laterally continuous).  |
|                            |  |                      |  | Lower  | Normally graded lapilli-tuff | 5 m, normally graded                    | Sequence of poorly-sorted beds containing subangular-rounded lapilli in both lithic- and pumice-rich lenses, with individual beds comprising 50-80 vol.% pumice (max size 12 cm), 5-20 vol.% lithics, and <5-45 vol.% ash.  | Primary high concentration PDC deposit (poor-sorting; lack of sedimentary structures).  |
| Old Road Bay Pumice        | Crops out on both the east and west coasts of Montserrat.              | N16.72899; E62.23521 | 13.1.1A, 11.1.1A, 4.2.3G, 9.2.1F, 9.2.1G, 9.2.1H | Upper  | Lapilli-tuff                 | 3.5 m, massive and normally graded      | Moderately-poorly sorted bed with rounded lapilli. Comprises 50 vol.% yellow pumices and lithics (difficult to distinguish due to weathering), and 50 vol.% coarse ash.   | Primary deposit of high concentration PDC (poorly sorted, heterogeneous, rounded clasts).   |
|                            |  |                      |  | Middle | Lapilli-tuff                 | <1 m, finely bedded                     | Alternating well-sorted ash and lapilli beds, with lamination in the ash layers. Coarser lapilli beds contain pumice and accretionary lapilli, with higher concentrations of pumice lapilli at the top of the unit.   | Primary tephra fall from pulsed eruption, or series of low-medium concentration density currents (well-sorted deposits).            |
|                            |  |                      |  | Lower  | Lapilli-tuff                 | 1.5 m, massive with normally graded top | Moderately sorted, with rounded lapilli dominated by yellow pumice (>90 vol.%; max size 7cm) and <10 vol.% white ash matrix.  | Primary pumice-rich low concentration PDC (homogenous, rounded clasts).   |
| South Lime Kiln Bay Pumice | Crops out within an isolated faulted block                             | N16.74799; E62.23473 | 11.1.4C  | Upper  | Lapilli-tuff                 | >2 m, reversely graded                  | Poorly-sorted, subangular-subrounded lapilli beds with variable proportions of pumice and lithic clasts, comprising 15-85 vol.% pumices (2cm mean size, max size 5 cm), 5-75 vol.% grey, black and purple lithics, and 10 vol.% buff ash. Better sorting in pumice-rich base; proportion of lithic clasts, and lithic clast size increases towards the top. | Primary deposit of high concentration PDC (heterogeneous, poorly sorted), possibly reworked at top.                                 |
|                            |  |                      |  | Middle | Lapilli-tuff                 | 4 m, massive                            | Sequence of thin beds with moderate-poor sorting of subangular-subrounded lapilli and slightly variable proportions of pumice and lithic clasts (75->95 vol.% pumice lapilli (2 cm mean size, max size 15 cm), 5-10 vol.% assorted lithics and <1-20 vol.% ash).  | Primary sequence of high concentration PDC deposits (poorly sorted units) and fall deposits (well sorted beds with angular clasts). |

|                             |  |                      |                           |       |              |                                    |  |  |
|-----------------------------|--|----------------------|---------------------------|-------|--------------|------------------------------------|--|--|
|                             |  |                      |                           | Lower | Lapilli-tuff | >1 m, massive                      | Poor-moderately sorted ash-rich beds with subangular pumice lapilli and lithic grains in variable proportions, comprising 5-30 vol.% pumice lapilli (2 cm mean size), 10-40 vol.% assorted lithics (3 cm mean size, max size 15 cm), and 60-90 vol.% coarse ash. The ash is red and comprises 30 vol.% plagioclase and pyroxene crystals. Fine-grained (weathered?) fiamme-shaped clasts also occur.   | Primary deposit of high concentration PDC (poor-moderate sorting, coarse lithics, high ash content). |
| <i>East of Centre Hills</i> |  |                      |                           |       |              |                                    |  |  |
| Statue Rock                 | Laterally traceable along the cliff at Statue rock                   | N16.78158; E62.17855 | 13.4.1E, 13.3.1D          | N/A   | Lapilli-tuff | 10 m, low-angle cross bedding      | Poorly sorted ash-rich deposit with rounded pumice lapilli and lithic lenses. Bedding defined by thin, elongate pumice lapilli lenses (one clast thickness). Total unit comprises 30 vol.% pumice lapilli (mean size 3 cm), 30 vol.% grey and black lithics (mean size 7 cm, max size ~1 m) and 40 vol.% coarse ash (containing ~30 vol.% pyroxene and plagioclase crystals).  | High concentration PDC deposits, potentially partially reworked.                                     |
| Bramble Pumice              | Crops out in isolated lenses (<50 m lateral extent)                  | N16.76603; E62.16407 | 14.1.2B, 15.1.3A, 16.1.4C | N/A   | Lapilli-tuff | 12 m, massive and reversely graded | Series of poorly-sorted lithic dominated units with subordinate lenses of angular-rounded pumice lapilli, often only one-clast thick. Pumices range in size from 1-5 cm, with variable proportions throughout the unit (5-30 vol.%, except in lenses), the remainder a mix of lithics (30-50 vol.% ) and grey or orange medium-coarse ash (up to 85 vol.% in parts). The ash is often crystal rich (up to 30 vol.% plagioclase and pyroxene crystals). The unit also contains 30-50 cm sized rip-up clasts of laminated ash. | Largely reworked deposit (rip-up clasts, poor sorting) derived from PDC deposits.                    |
| Angry Bird Pumice           | Traceable along much of the east coast, less continuous to the south | N16.77051; E62.16901 | 14.1.2.A, 13.1.2B         | N/A   | lapilli-tuff | 4.5 m, massive and normally graded | Series of up to 4 units separated by lithic breccias. Moderately-well sorted beds of angular-subangular pumice lapilli. Pumices have a flattened shape and have mostly altered to clays. Beds comprise 85 vol.% white pumice (1 cm mean size, max size 3 cm), 5 vol.% grey and red lithics, and 10 vol.% pink coarse ash. The ash is crystal rich, consisting of 50 vol.% plagioclase and pyroxene crystals.   | Primary tephra fall deposits (well-sorted, homogenous, angular clasts).                              |

1074  
1075  
1076

**Table 2: Whole-rock major element analyses of pumice from pyroclastic units in central Montserrat (XRF, wt.%, normalised to 100% anhydrous compositions).**

| Sample     | Unit           | SiO <sub>2</sub> | TiO <sub>2</sub> | Al <sub>2</sub> O <sub>3</sub> | Fe <sub>2</sub> O <sub>3</sub> | MnO  | MgO  | CaO  | K <sub>2</sub> O | Na <sub>2</sub> O | P <sub>2</sub> O <sub>5</sub> | Mg#   |
|------------|----------------|------------------|------------------|--------------------------------|--------------------------------|------|------|------|------------------|-------------------|-------------------------------|-------|
| 3.1.8C     | Attic          | 65.39            | 0.42             | 16.72                          | 5.13                           | 0.14 | 1.99 | 5.77 | 1.12             | 3.22              | 0.11                          | 60.61 |
| 8.1.1A     | Attic          | 65.36            | 0.41             | 16.37                          | 5.32                           | 0.16 | 2.13 | 5.49 | 1.10             | 3.54              | 0.12                          | 61.30 |
| 3.1.2 A +B | Woodlands Bay  | 62.27            | 0.54             | 17.77                          | 6.23                           | 0.15 | 2.38 | 6.44 | 0.91             | 3.26              | 0.05                          | 60.22 |
| 5.1.1B     | Woodlands Bay  | 61.33            | 0.61             | 17.64                          | 6.88                           | 0.16 | 2.51 | 6.57 | 0.91             | 3.29              | 0.10                          | 59.04 |
| 3.4.2H     | Bunkum Bay     | 62.87            | 0.46             | 17.56                          | 5.58                           | 0.14 | 2.30 | 6.25 | 1.04             | 3.73              | 0.09                          | 61.98 |
| 13.4.1E    | Statue Rock    | 58.66            | 0.59             | 19.38                          | 7.68                           | 0.18 | 2.46 | 6.95 | 0.60             | 3.40              | 0.10                          | 55.96 |
| BP 1       | Bransby Point  | 61.60            | 0.53             | 17.65                          | 6.79                           | 0.16 | 2.24 | 6.77 | 0.90             | 3.26              | 0.13                          | 56.63 |
| BP 2       | Bransby Point  | 59.14            | 0.53             | 17.45                          | 7.02                           | 0.18 | 2.87 | 7.07 | 0.87             | 4.34              | 0.15                          | 61.82 |
| 7.1.1A     | Garibaldi Hill | 60.90            | 0.55             | 18.81                          | 6.65                           | 0.15 | 2.48 | 6.34 | 0.83             | 3.22              | 0.06                          | 59.64 |

|          |                        |       |      |       |       |      |      |      |      |      |      |       |
|----------|------------------------|-------|------|-------|-------|------|------|------|------|------|------|-------|
| 5.2.3 E  | Garibaldi Hill         | 60.98 | 0.56 | 17.51 | 6.98  | 0.18 | 2.52 | 6.96 | 0.80 | 3.35 | 0.16 | 58.88 |
| 15.1.3A  | Bramble                | 62.27 | 0.54 | 17.74 | 6.22  | 0.15 | 2.36 | 6.46 | 0.91 | 3.29 | 0.05 | 60.09 |
| 4.2.3G   | Old Road Bay<br>pumice | 61.04 | 0.56 | 17.76 | 6.60  | 0.17 | 2.52 | 6.78 | 0.86 | 3.55 | 0.17 | 60.15 |
| 9.2.1 G  | Old Road Bay<br>pumice | 59.86 | 0.57 | 19.15 | 6.69  | 0.15 | 2.45 | 6.93 | 0.70 | 3.44 | 0.07 | 59.17 |
| 13.1.1 A | Old Road Bay<br>pumice | 60.91 | 0.54 | 17.64 | 6.71  | 0.17 | 2.59 | 6.96 | 0.85 | 3.50 | 0.14 | 60.42 |
| 13.1.2 B | Angry Bird             | 52.30 | 0.84 | 21.29 | 10.42 | 0.32 | 4.59 | 7.41 | 0.24 | 2.46 | 0.13 | 63.58 |
| 11.1.4C  | South Lime Kiln<br>Bay | 61.98 | 0.51 | 17.43 | 6.43  | 0.18 | 2.53 | 6.58 | 0.78 | 3.42 | 0.15 | 60.94 |
| 9.1.2 A  | un-named               | 62.13 | 0.51 | 17.87 | 6.00  | 0.17 | 2.25 | 6.48 | 0.92 | 3.60 | 0.08 | 59.80 |
| 2.1.2 A  | un-named               | 59.22 | 0.56 | 19.02 | 7.40  | 0.19 | 2.62 | 6.75 | 0.72 | 3.40 | 0.11 | 58.40 |
| 7.3.2C   | un-named               | 61.94 | 0.53 | 17.90 | 6.06  | 0.15 | 2.28 | 6.77 | 0.91 | 3.36 | 0.11 | 59.87 |
| 5.2.1 D  | un-named               | 58.27 | 0.86 | 15.30 | 9.45  | 0.21 | 4.99 | 7.14 | 1.16 | 2.44 | 0.17 | 67.65 |
| 9.2.1 E  | un-named               | 58.21 | 0.68 | 19.38 | 9.32  | 0.17 | 2.99 | 5.89 | 0.28 | 3.00 | 0.09 | 55.93 |
| 12.1.4 B | un-named               | 56.80 | 0.72 | 18.67 | 7.42  | 0.14 | 3.45 | 8.54 | 0.90 | 3.23 | 0.11 | 64.82 |
| 16.1.2 A | un-named               | 60.19 | 0.52 | 17.86 | 6.52  | 0.16 | 2.56 | 6.83 | 0.84 | 4.38 | 0.14 | 60.82 |

1077  
1078

**Table 3: Whole rock trace element chemistry of pumice from pyroclastic units in central Montserrat (solution ICP-MS, ppm)**

| Sample        | Unit             | Y     | Sr    | Ta    | Nb    | La    | Ce    | Pr    | Nd    | Sm    | Eu    | Dy    | Ho    | Er    | Tm    | Yb    | Lu    | Hf    | Th    |
|---------------|------------------|-------|-------|-------|-------|-------|-------|-------|-------|-------|-------|-------|-------|-------|-------|-------|-------|-------|-------|
| 3.2.1F        | Attic            | 15.28 | 253.8 | 0.349 | 3.166 | 11.55 | 22.86 | 3.026 | 11.71 | 2.395 | 0.817 | 2.304 | 0.504 | 1.511 | 0.243 | 1.692 | 0.281 | 2.09  | 2.869 |
| 8.1.1A        | Attic            | 16.05 | 256.9 | 0.614 | 3.501 | 12.85 | 26.72 | 3.26  | 12.5  | 2.519 | 0.811 | 2.369 | 0.515 | 1.552 | 0.252 | 1.808 | 0.303 | 2.243 | 3.325 |
| 3.1.8C        | Attic            | 17.05 | 277.8 | 0.412 | 3.289 | 12.66 | 26.48 | 3.236 | 12.59 | 2.625 | 0.83  | 2.518 | 0.545 | 1.628 | 0.261 | 1.843 | 0.311 | 3.097 | 3.921 |
| 10.1.1 A      | Woodlands<br>Bay | 22.36 | 241.1 | 0.441 | 3.361 | 10.84 | 22.96 | 3.138 | 12.87 | 2.933 | 0.961 | 3.323 | 0.73  | 2.206 | 0.361 | 2.593 | 0.429 | 3.399 | 3.339 |
| 3.1.2 A<br>+B | Woodlands<br>Bay | 21.83 | 251.5 | 0.3   | 2.985 | 10.77 | 22.73 | 3.05  | 12.83 | 2.924 | 0.932 | 3.215 | 0.695 | 2.103 | 0.338 | 2.381 | 0.385 | 3.305 | 2.878 |
| 5.1.1B        | Woodlands<br>Bay | 21.07 | 250.8 | 0.38  | 3.04  | 10.87 | 24.32 | 3.105 | 12.75 | 2.904 | 0.935 | 3.197 | 0.692 | 2.086 | 0.334 | 2.338 | 0.38  | 3.03  | 2.75  |
| 5.1.1A        | Woodlands<br>Bay | 21.66 | 239.4 | 0.291 | 3.087 | 10.53 | 23.12 | 3.09  | 12.87 | 2.989 | 0.935 | 3.307 | 0.727 | 2.148 | 0.347 | 2.435 | 0.401 | 2.867 | 2.46  |
| 3.4.2H        | Bunkum<br>Bay    | 15.99 | 249   | 0.713 | 2.72  | 11.04 | 21.19 | 3.078 | 12.23 | 2.587 | 0.809 | 2.501 | 0.525 | 1.529 | 0.243 | 1.717 | 0.274 | 1.855 | 2.606 |
| 6.1.2 A       | Bunkum<br>Bay    | 18    | 216.8 | 0.304 | 2.928 | 9.446 | 20.74 | 2.918 | 12.18 | 2.734 | 0.83  | 2.934 | 0.628 | 1.879 | 0.297 | 2.089 | 0.338 | 2.566 | 2.003 |
| 4.2.5I        | Foxes Bay        | 28.05 | 260.7 | 0.357 | 3.352 | 12.34 | 27.04 | 3.71  | 15.64 | 3.643 | 1.101 | 4.144 | 0.919 | 2.729 | 0.436 | 3.052 | 0.491 | 3.31  | 2.941 |
| 13.4.1E       | Statue<br>Rock   | 27.29 | 235.3 | 0.297 | 2.808 | 9.906 | 21.56 | 3.21  | 13.81 | 3.306 | 1.063 | 3.954 | 0.861 | 2.599 | 0.404 | 2.736 | 0.45  | 2.885 | 2.187 |
| 2.1.2B        | Old Road         | 17.38 | 284.3 | 0.357 | 2.64  | 10.2  | 22.04 | 2.753 | 11.09 | 2.458 | 0.849 | 2.611 | 0.57  | 1.692 | 0.276 | 1.889 | 0.305 | 1.927 | 2.214 |

| <b>Bay tuff</b> |                            |       |       |       |       |       |       |       |       |       |       |       |       |       |       |       |       |       |       |
|-----------------|----------------------------|-------|-------|-------|-------|-------|-------|-------|-------|-------|-------|-------|-------|-------|-------|-------|-------|-------|-------|
| <b>9.2.1 C</b>  | <b>Garibaldi Hill</b>      | 25.91 | 235.5 | 0.528 | 3.17  | 11.61 | 24.36 | 3.542 | 14.77 | 3.467 | 0.997 | 3.823 | 0.836 | 2.515 | 0.404 | 2.828 | 0.46  | 3.009 | 2.693 |
| <b>7.1.1A</b>   | <b>Garibaldi Hill</b>      | 24.55 | 238.7 | 1.684 | 3.132 | 12.21 | 23.49 | 3.544 | 15.08 | 3.42  | 1.018 | 3.696 | 0.806 | 2.388 | 0.383 | 2.699 | 0.439 | 3.04  | 2.754 |
| <b>4.1.4H</b>   | <b>Garibaldi Hill</b>      | 24.98 | 271.4 | 0.337 | 3.08  | 10.47 | 24.18 | 3.272 | 13.9  | 3.353 | 1.059 | 3.88  | 0.843 | 2.534 | 0.401 | 2.832 | 0.452 | 2.838 | 2.098 |
| <b>5.2.3 E</b>  | <b>Garibaldi Hill</b>      | 25.01 | 278.8 | 1.312 | 3.095 | 11.34 | 25.48 | 3.373 | 14.23 | 3.362 | 1.089 | 3.754 | 0.824 | 2.478 | 0.393 | 2.701 | 0.438 | 3.235 | 2.465 |
| <b>11.1.3 B</b> | <b>Garibaldi Hill</b>      | 26.5  | 261.8 | 0.29  | 2.713 | 12.61 | 24.58 | 3.483 | 14.71 | 3.308 | 1.006 | 3.927 | 0.856 | 2.542 | 0.402 | 2.77  | 0.439 | 2.655 | 2.357 |
| <b>15.1.3A</b>  | <b>Bramble</b>             | 22.31 | 246.8 | 0.335 | 2.725 | 10.1  | 22.67 | 3.113 | 13.19 | 3.064 | 0.955 | 3.404 | 0.727 | 2.187 | 0.352 | 2.417 | 0.389 | 2.651 | 2.033 |
| <b>16.1.4C</b>  | <b>Bramble</b>             | 19.41 | 256.1 | 0.943 | 2.605 | 9.011 | 20.2  | 2.855 | 12.23 | 2.875 | 0.936 | 3.016 | 0.64  | 1.906 | 0.306 | 2.104 | 0.337 | 2.387 | 1.744 |
| <b>14.1.2 B</b> | <b>Bramble</b>             | 20.38 | 211.6 | 0.473 | 2.7   | 9.841 | 21.9  | 2.886 | 12    | 2.741 | 0.84  | 3.056 | 0.667 | 2.009 | 0.324 | 2.223 | 0.352 | 2.673 | 2.31  |
| <b>9.2.1 H</b>  | <b>Old Road Bay</b>        | 21.71 | 244.4 | 0.269 | 2.431 | 9.483 | 20.34 | 2.886 | 12.13 | 2.906 | 0.87  | 3.303 | 0.709 | 2.116 | 0.332 | 2.305 | 0.37  | 2.568 | 2.15  |
| <b>9.2.1F</b>   | <b>Old Road Bay</b>        | 20.25 | 257.2 | 0.268 | 2.805 | 9.332 | 21.27 | 2.808 | 12.13 | 2.9   | 0.968 | 3.172 | 0.678 | 2.02  | 0.327 | 2.279 | 0.36  | 2.866 | 2.09  |
| <b>9.2.1 G</b>  | <b>Old Road Bay</b>        | 20.97 | 301   | 0.27  | 2.865 | 8.883 | 19.99 | 2.639 | 11.38 | 2.821 | 0.969 | 3.219 | 0.711 | 2.126 | 0.347 | 2.431 | 0.393 | 3.077 | 2.213 |
| <b>11.1.1A</b>  | <b>Old Road Bay</b>        | 19.56 | 220.9 | 0.414 | 2.684 | 10.12 | 22.28 | 2.835 | 11.64 | 2.645 | 0.839 | 2.975 | 0.64  | 1.934 | 0.312 | 2.192 | 0.354 | 2.73  | 2.536 |
| <b>4.2.3G</b>   | <b>Old Road Bay</b>        | 20.35 | 233   | 1.315 | 2.721 | 8.985 | 20.67 | 2.789 | 11.95 | 2.841 | 0.912 | 3.306 | 0.706 | 2.139 | 0.343 | 2.393 | 0.387 | 2.04  | 1.569 |
| <b>13.1.2 B</b> | <b>Angry Bird</b>          | 34.8  | 236.7 | 0.549 | 3.751 | 15.06 | 26.34 | 4.322 | 18.38 | 4.592 | 1.407 | 5.567 | 1.175 | 3.43  | 0.536 | 3.686 | 0.576 | 3.285 | 2.971 |
| <b>11.1.4C</b>  | <b>South Lime Kiln Bay</b> | 33.89 | 262.8 | 0.284 | 2.944 | 10.64 | 24.43 | 3.606 | 16.42 | 4.157 | 1.189 | 4.828 | 1.036 | 3.104 | 0.482 | 3.296 | 0.517 | 2.885 | 2.202 |
| <b>9.1.2 A</b>  | un-named                   | 31.07 | 236.9 | 0.351 | 3.001 | 11.1  | 23.33 | 3.822 | 17.43 | 4.261 | 1.223 | 4.613 | 1.023 | 3.181 | 0.525 | 3.794 | 0.639 | 2.871 | 2.577 |
| <b>7.3.2C</b>   | un-named                   | 29.41 | 232.9 | 0.406 | 2.954 | 15.09 | 23.41 | 4.51  | 19.57 | 4.34  | 1.282 | 4.352 | 0.953 | 2.768 | 0.442 | 3.011 | 0.483 | 2.63  | 2.505 |
| <b>12.1.6C</b>  | un-named                   | 18.39 | 226.7 | 0.441 | 2.823 | 8.002 | 17.36 | 2.299 | 9.956 | 2.408 | 0.88  | 2.832 | 0.614 | 1.851 | 0.296 | 2.098 | 0.337 | 2.804 | 2.058 |
| <b>16.1.5D</b>  | un-named                   | 20.69 | 223.6 | 0.237 | 2.526 | 9.436 | 20.74 | 2.952 | 12.72 | 2.94  | 0.895 | 3.169 | 0.677 | 1.997 | 0.328 | 2.224 | 0.357 | 2.424 | 1.866 |
| <b>2.1.2 A</b>  | un-named                   | 20.73 | 282.8 | 0.306 | 2.834 | 9.032 | 20.96 | 2.894 | 12.7  | 2.999 | 1.057 | 3.231 | 0.692 | 2.062 | 0.329 | 2.26  | 0.37  | 2.812 | 1.93  |
| <b>4.2.3F</b>   | un-named                   | 21.97 | 273.1 | 1.25  | 2.493 | 9.313 | 21.21 | 2.907 | 12.66 | 3.143 | 1.004 | 3.502 | 0.741 | 2.224 | 0.346 | 2.335 | 0.364 | 2.484 | 1.899 |
| <b>16.1.2 A</b> | un-named                   | 16.3  | 196.6 | 0.22  | 2.315 | 7.361 | 16.85 | 2.247 | 9.385 | 2.245 | 0.738 | 2.522 | 0.545 | 1.669 | 0.262 | 1.848 | 0.305 | 2.093 | 1.534 |
| <b>9.2.1 E</b>  | un-named                   | 16.27 | 224.3 | 0.354 | 2.858 | 7.178 | 19.18 | 2.408 | 10.34 | 2.492 | 1.131 | 2.69  | 0.56  | 1.647 | 0.262 | 1.861 | 0.299 | 2.274 | 1.818 |
| <b>12.1.1A</b>  | un-named                   | 16.08 | 326.7 | 0.321 | 1.531 | 6.008 | 13.24 | 1.778 | 7.862 | 2.082 | 0.771 | 2.7   | 0.569 | 1.612 | 0.24  | 1.594 | 0.242 | 1.18  | 1.242 |

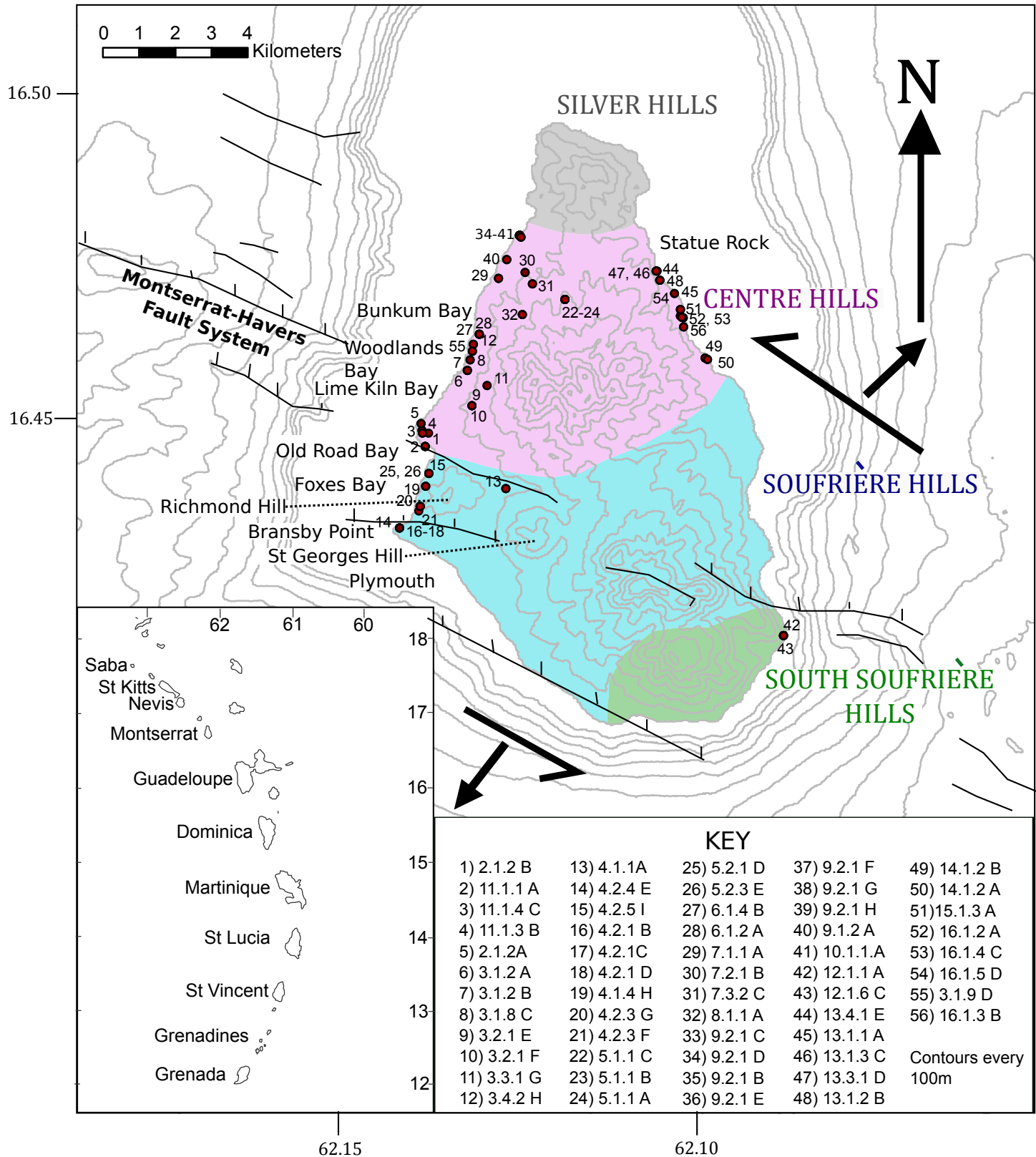
1079  
1080

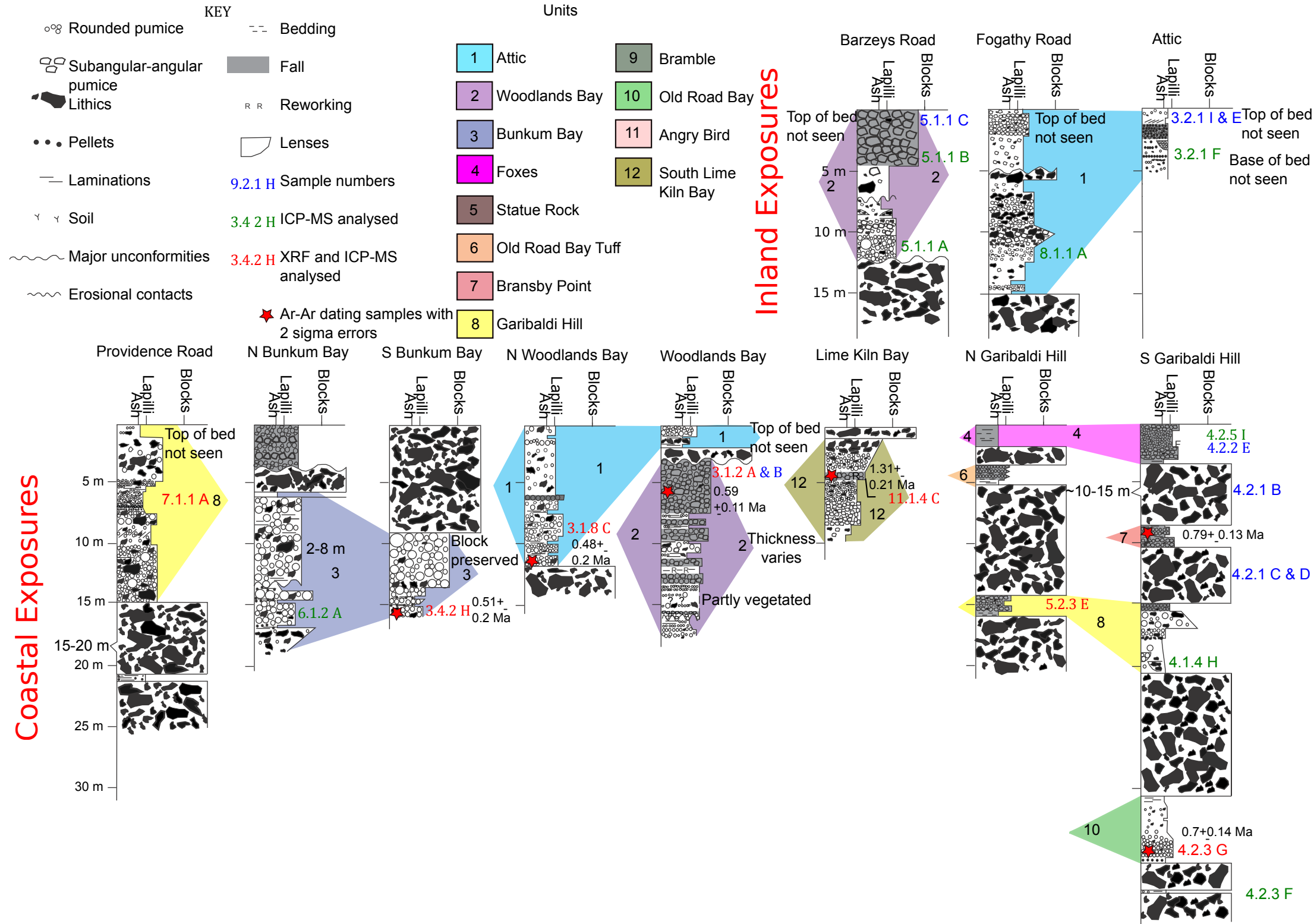
**Table 4: Estimated minimum deposit volumes (tephra volume) for selected fall deposits (cf. Pyle, 1999)**

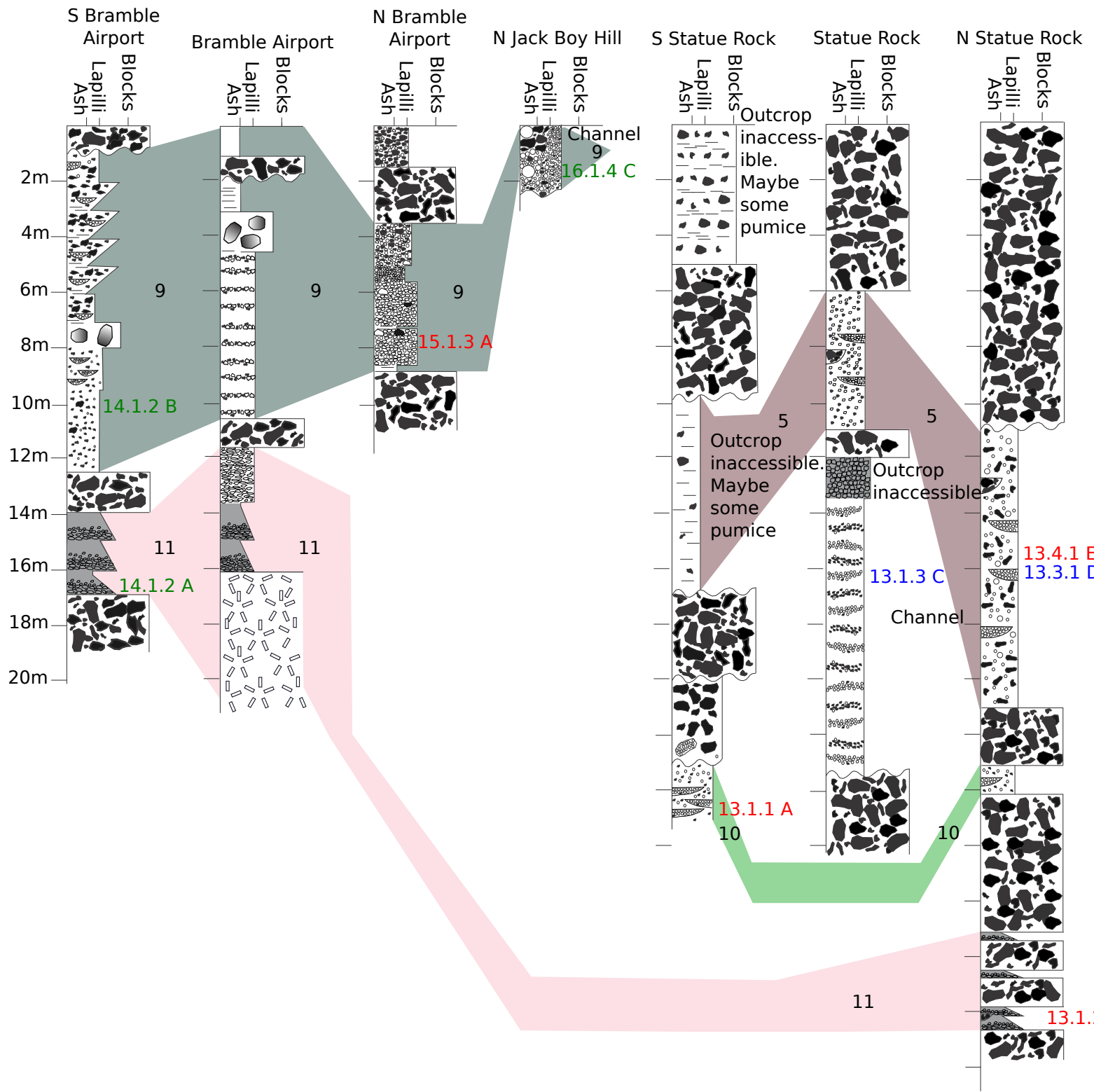
| <b>Unit</b> | <b>Isopach</b> | <b>Isopach</b> | <b>Deposit</b> |
|-------------|----------------|----------------|----------------|
|-------------|----------------|----------------|----------------|

|                            | <b>thickness<br/>(m)</b> | <b>area (km<sup>2</sup>)</b> | <b>volume<br/>(km<sup>3</sup>)</b> |
|----------------------------|--------------------------|------------------------------|------------------------------------|
| <b>Attic</b>               | 0.3                      | 20                           | 0.02                               |
| <b>Woodlands Bay</b>       | 4                        | 29                           | 0.43                               |
| <b>Old Road Bay tuff</b>   | 0.6                      | 19                           | 0.04                               |
| <b>Bransby Point</b>       | 1                        | 63                           | 0.23                               |
| <b>Garibaldi Hill</b>      | 0.6                      | 62                           | 0.14                               |
| <b>Old Road Bay pumice</b> | 0.3                      | 30                           | 0.03                               |
| <b>Angry Bird</b>          | 1                        | 49                           | 0.18                               |

1081







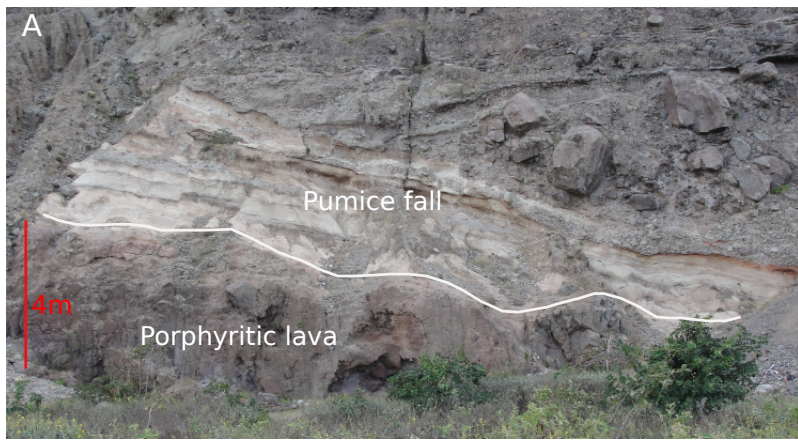
**KEY**

- 13.1.3 C Sample numbers
- 14.1.2 B ICP-MS analysed samples
- 13.1.1 A XRF and ICP-MS analysed samples

- Rounded pumice
- Subangular- angular pumice
- Lithics
- Pellets
- Laminations
- Unconformities
- Lava
- Fall
- Ash rip-up clasts
- Pumice rip-up clasts
- Lenses

**Units**

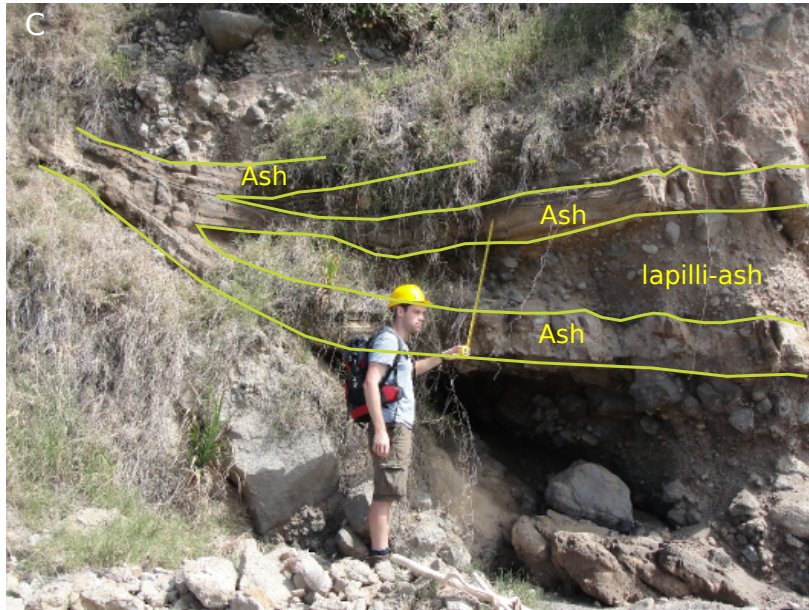
- |                     |                        |
|---------------------|------------------------|
| 1 Attic             | 7 Bransby Point        |
| 2 Woodlands Bay     | 8 Garibaldi Hill       |
| 3 Bunkum Bay        | 9 Bramble              |
| 4 Foxes             | 10 Old Road Bay        |
| 5 Statue Rock       | 11 Angry Bird          |
| 6 Old Road Bay Tuff | 12 South Lime Kiln Bay |



N 16.77051, W 62.16901  
 Angry Bird pumice



N 16.72365, W 62.24035  
 Bransby Point pumice



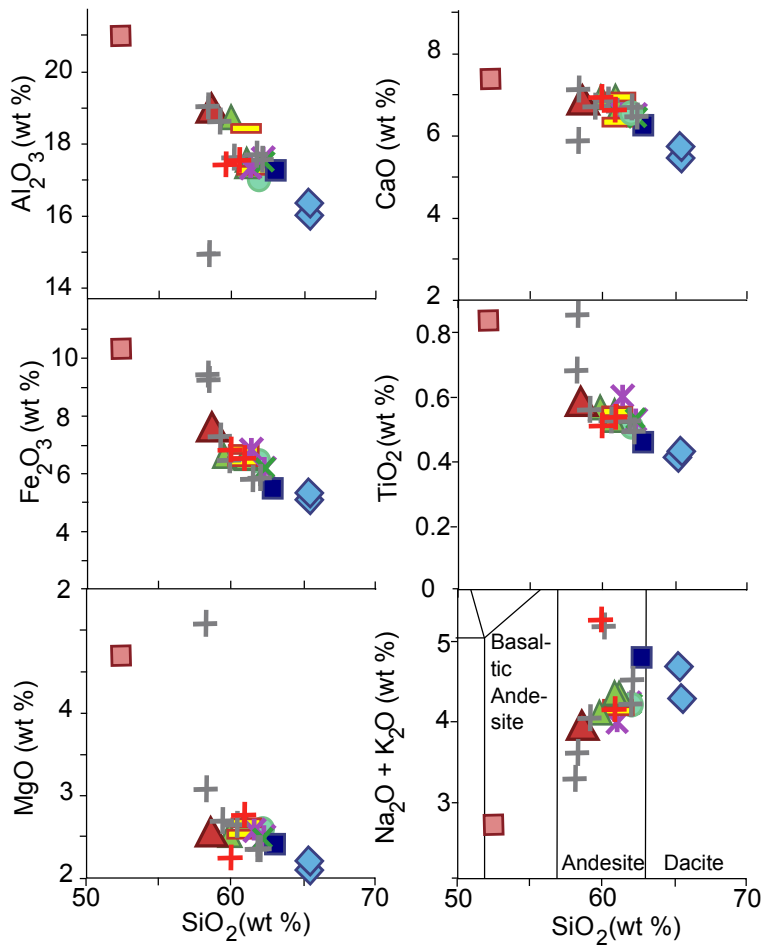
N 16.76946, W 62.22195  
 Bunkum Bay pumice



N 16.76298, W 62.22343  
 Woodlands pumice

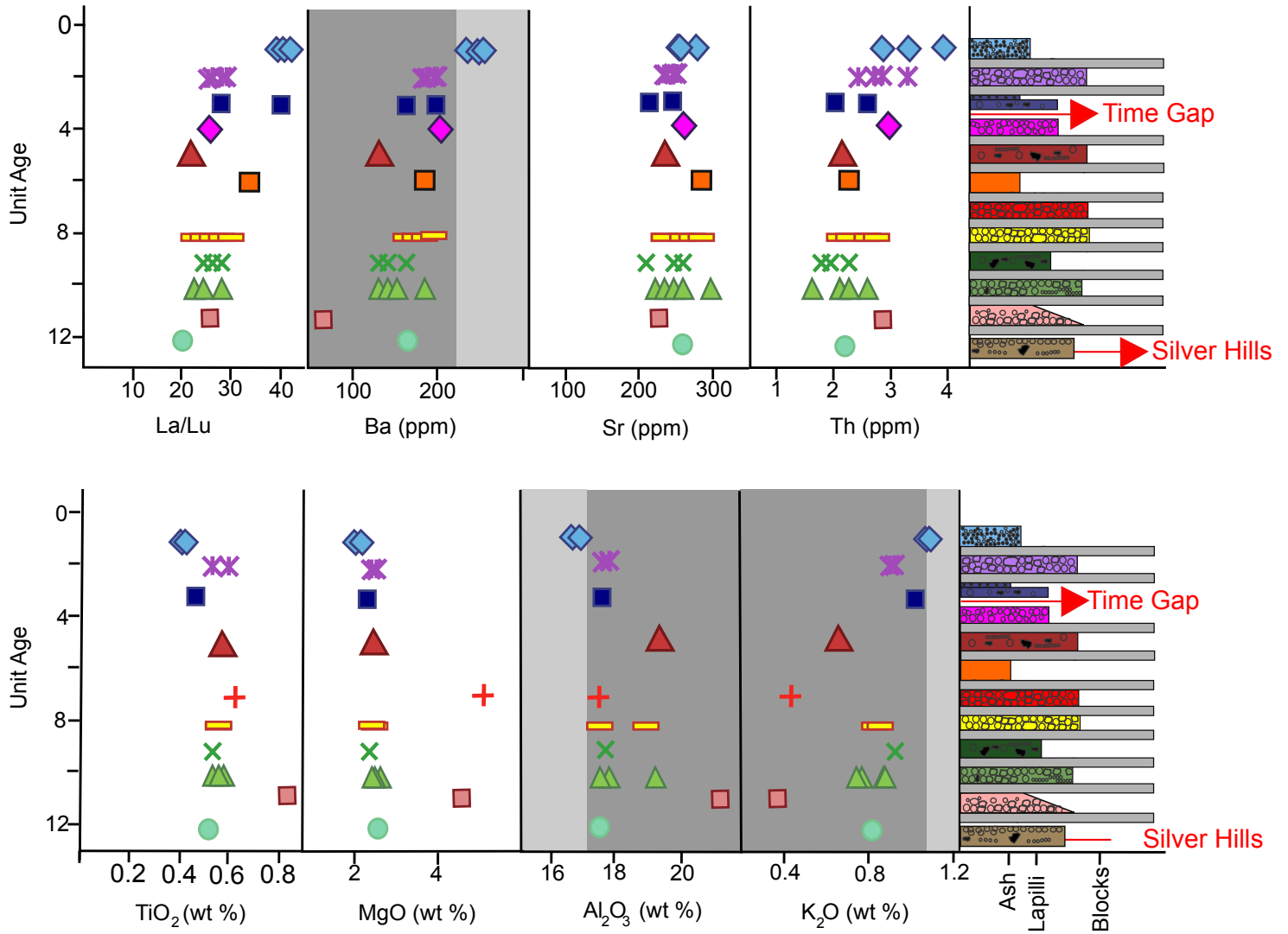


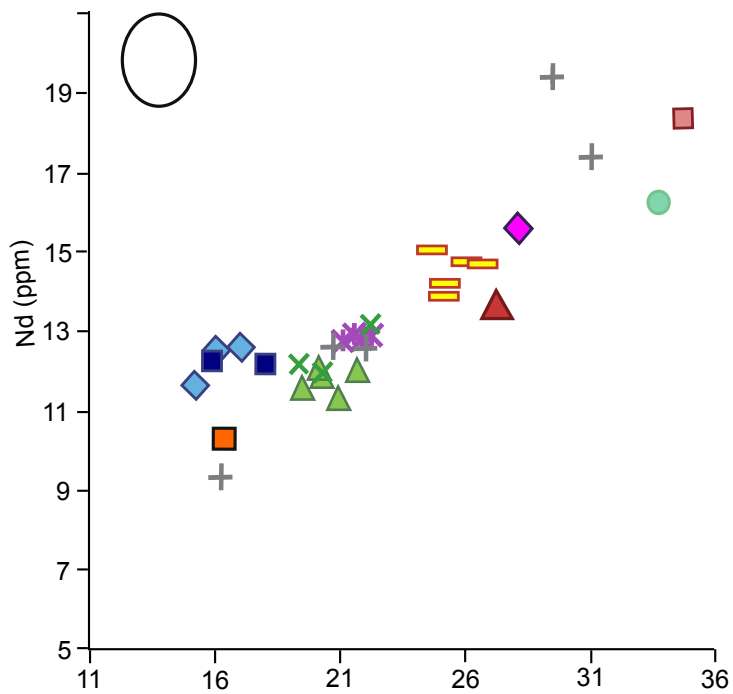
N 16.75413, W 62.22226  
 Attic pumice



**KEY**

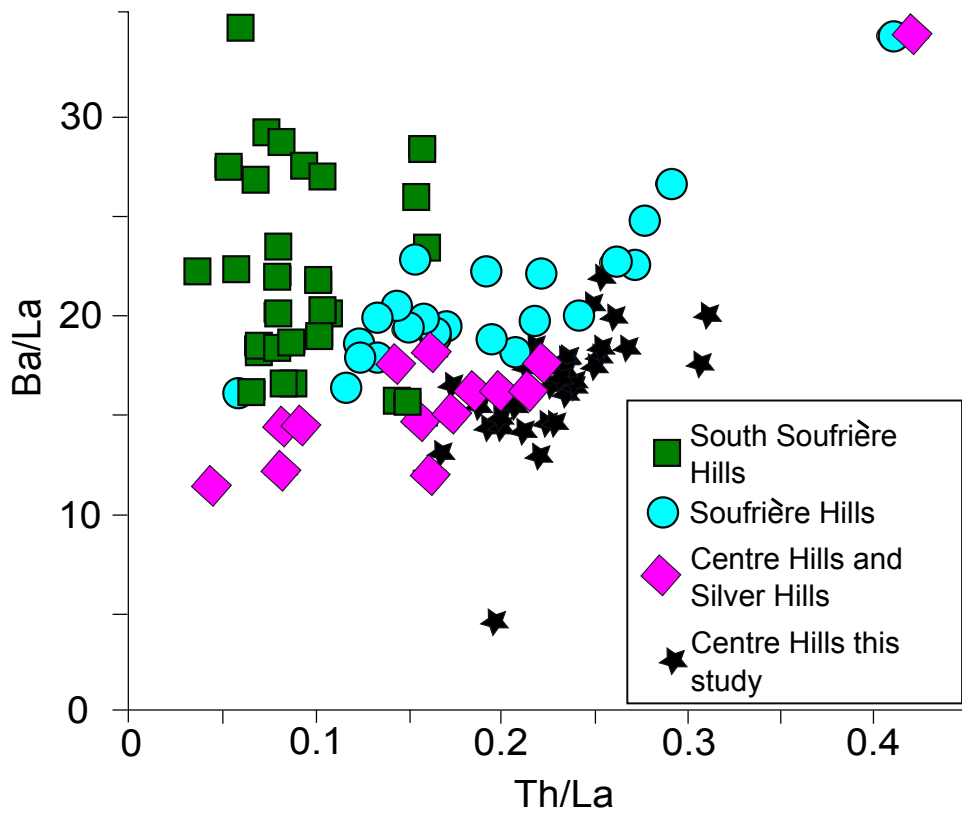
- |                 |                       |
|-----------------|-----------------------|
| ◆ Attic         | ▬ Garibaldi Hill      |
| ✱ Woodlands Bay | ✕ Bramble             |
| ■ Bunkum Bay    | ▲ Old Road Bay        |
| ▲ Statue Rock   | ■ Angry Bird          |
| ✚ Bransby Point | ● South Lime Kiln Bay |
|                 | ✚ Undifferentiated    |

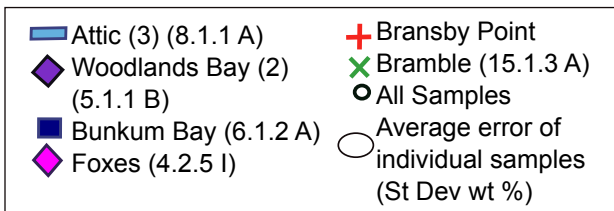
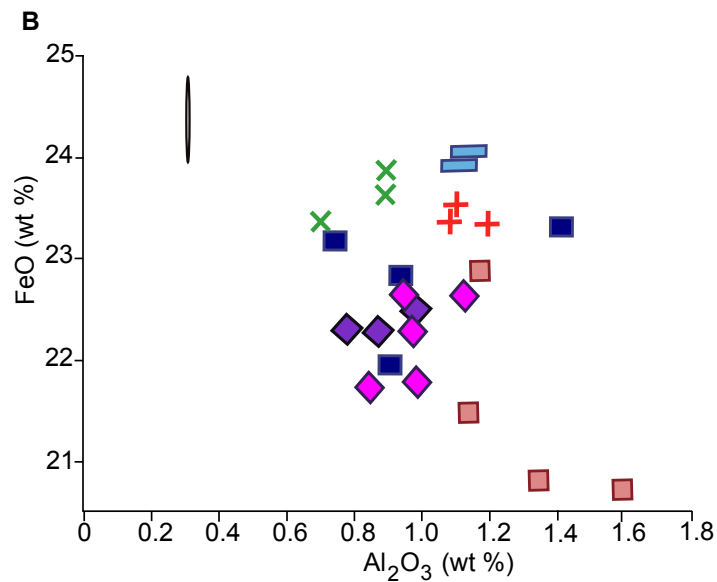
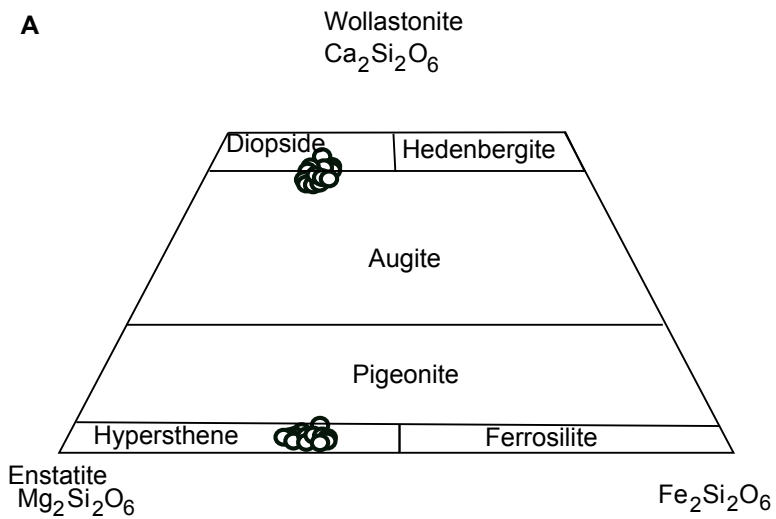


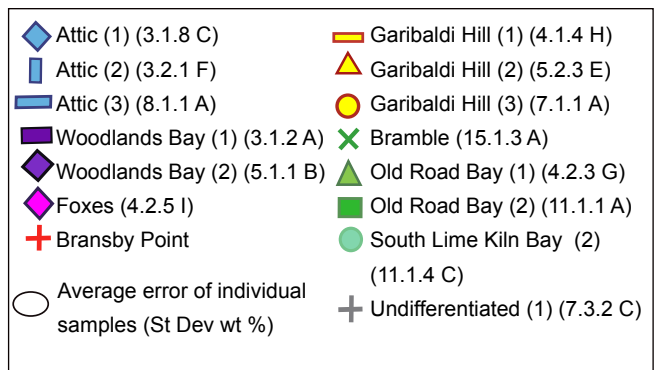
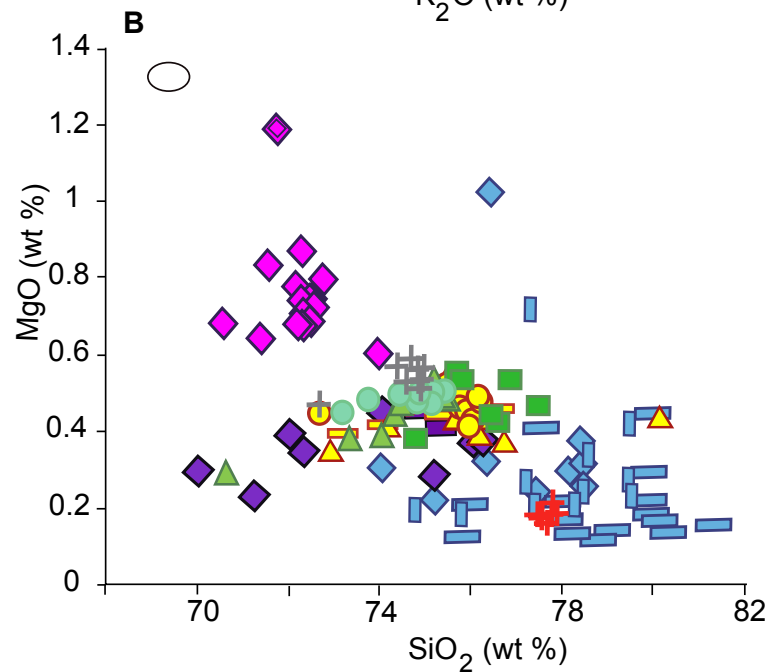
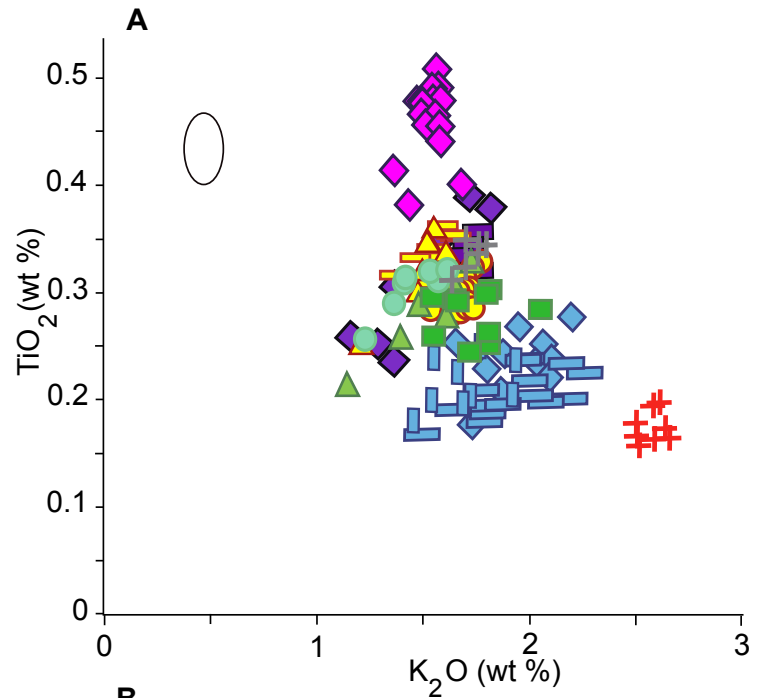


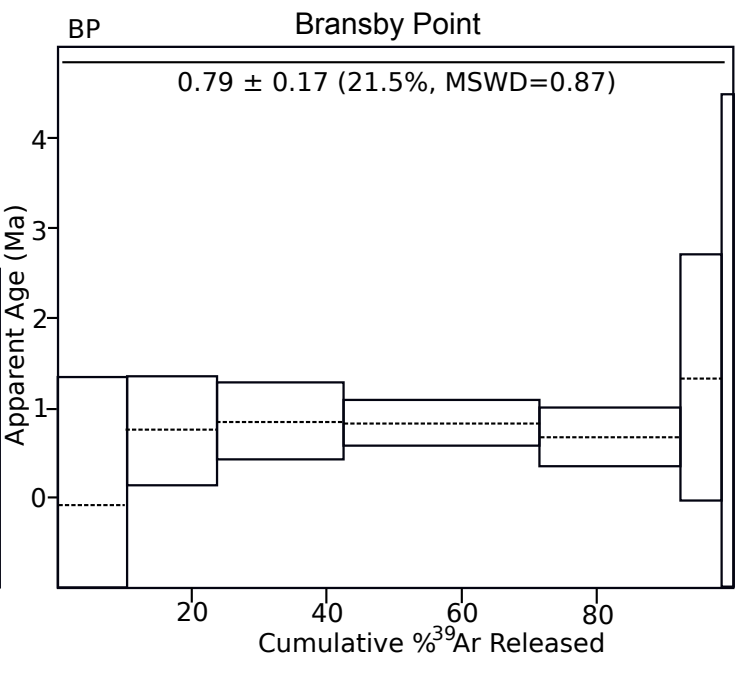
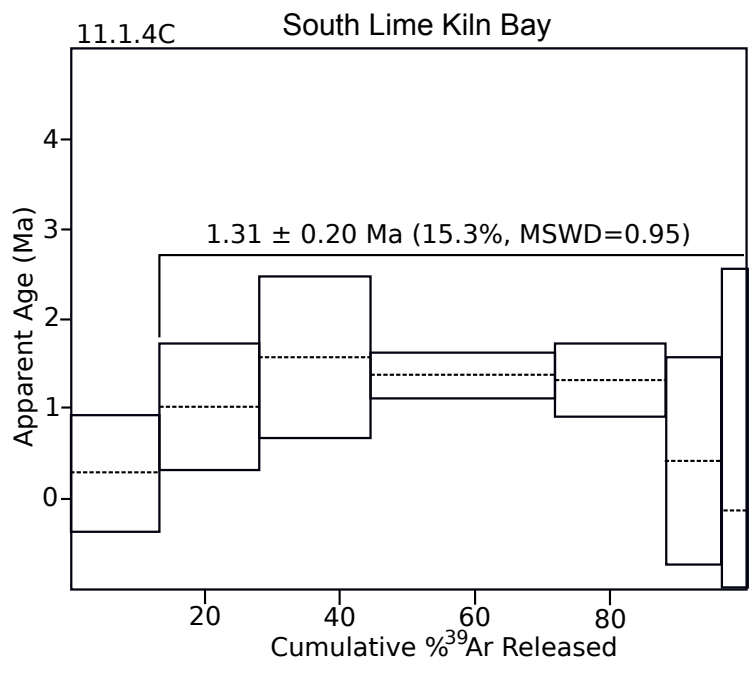
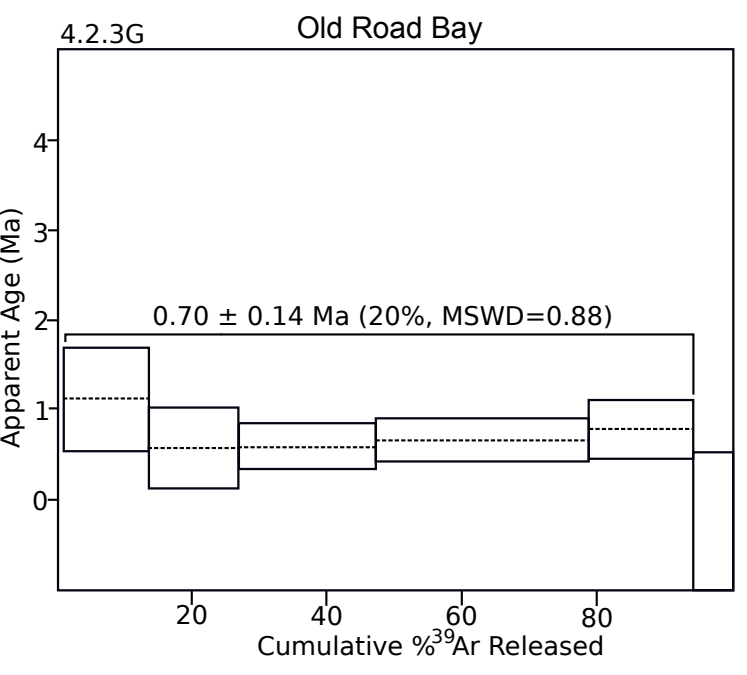
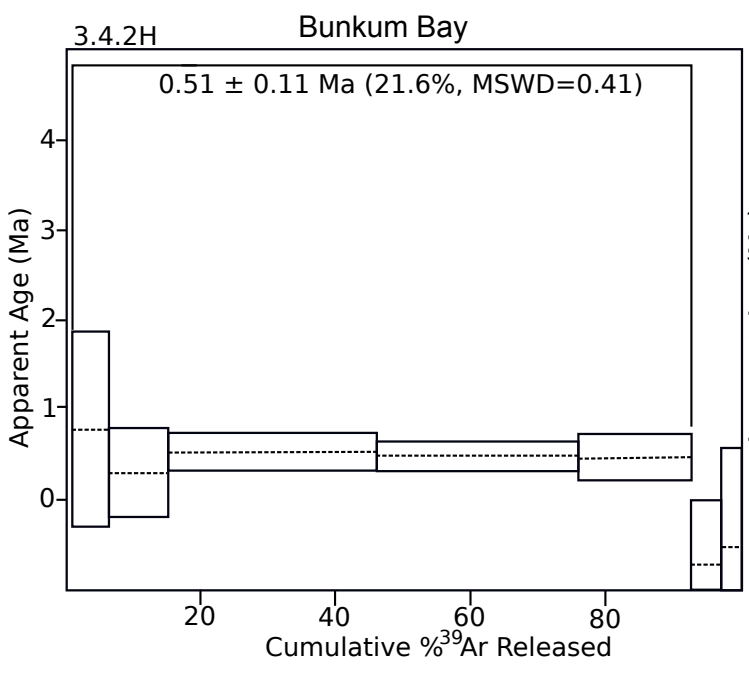
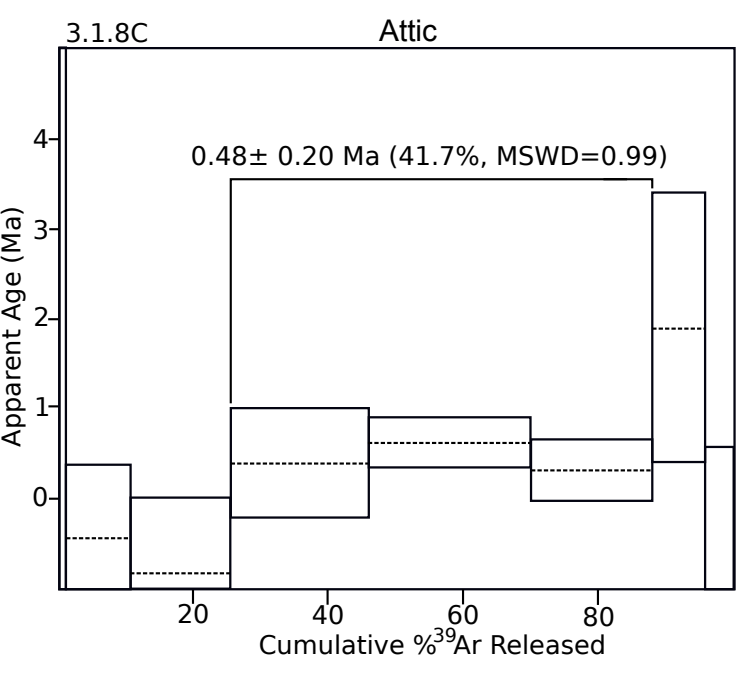
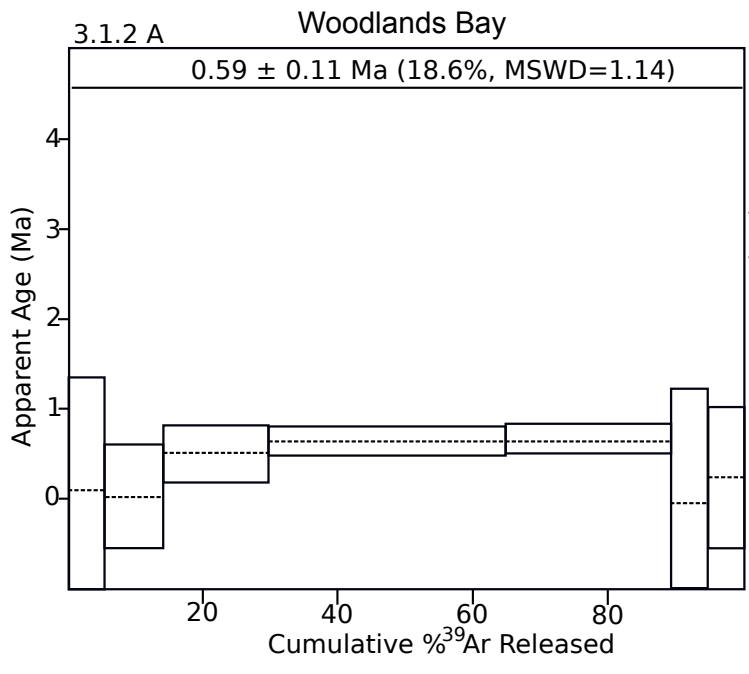
**KEY**

- ◆ Attic
- ✕ Woodlands Bay
- Bunkum Bay
- ◆ Foxes
- ▲ Statue Rock
- Old Road Bay Tuff
- ▬ Garibaldi Hill
- ✕ Bramble
- ▲ Old Road Bay
- Angry Bird
- South Lime Kiln Bay
- + Undifferentiated
- Maximum error ellipse (± 1 st dev)

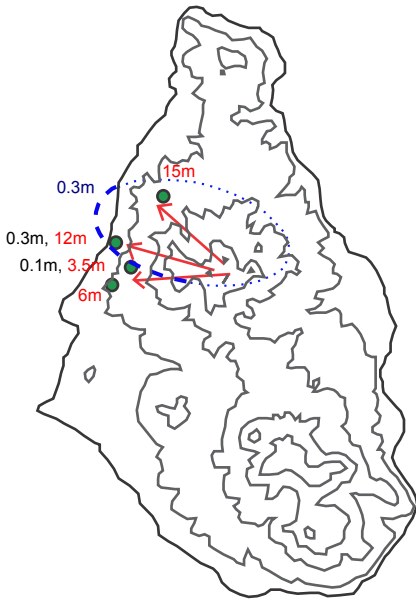




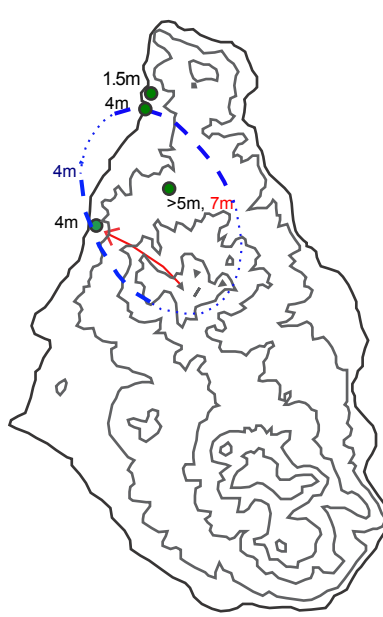




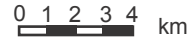
Attic tephra  
0.48 ± 0.2 Ma



Woodlands tephra  
0.59 ± 0.11 Ma



KEY



10m Pyroclastic density current deposit thickness

1.3m Fall thickness

50cm Isopach thickness

● Site of thickness measurement

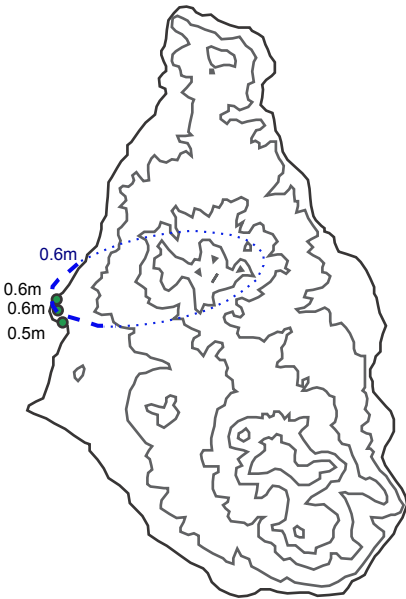
→ Flow direction

--- Moderately constrained isopach

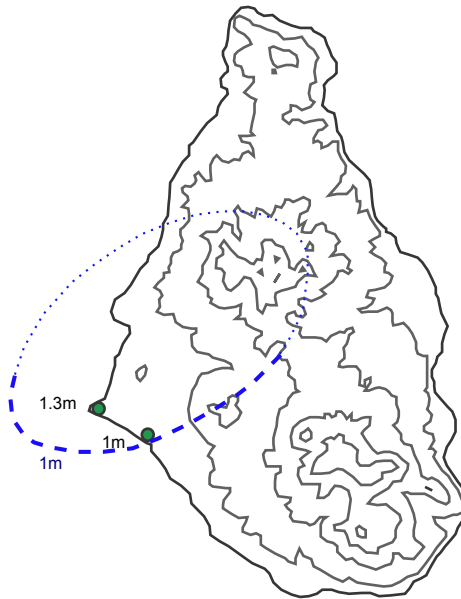
..... Poorly constrained isopach

— Contours at 200m intervals

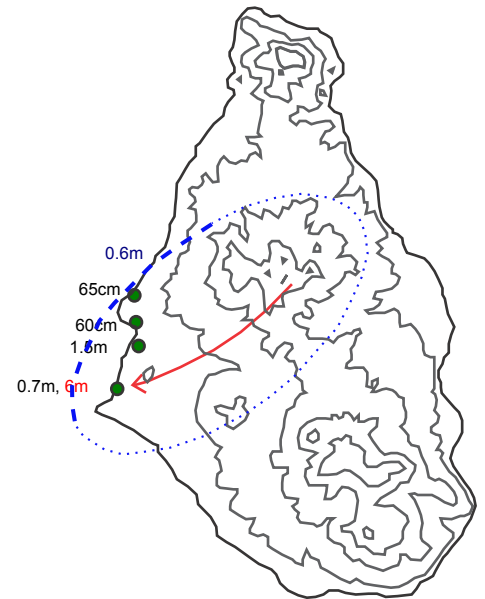
Old Road Bay Tuff



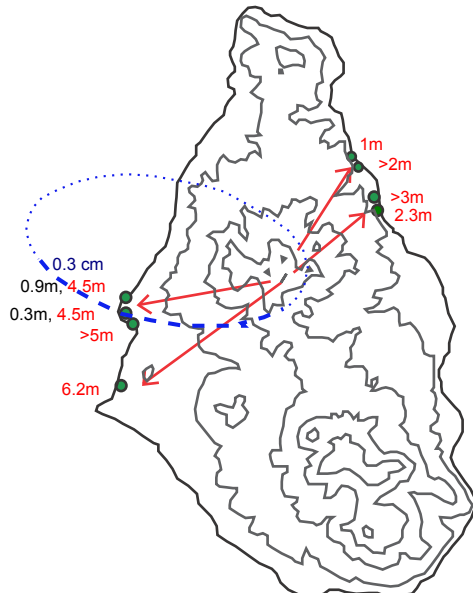
Bransby Point tephra  
0.79 ± 0.13 Ma



Garibaldi Hill tephra



Old Road Bay tephra  
0.7 ± 0.14 Ma



Angry Bird tephra  
(4 similar magnitude events)

